

Fourier Transform Emission Spectroscopy of the $g^4\Delta - a^4\Delta$ System of FeF

R. S. Ram,* P. F. Bernath,*¹ and S. P. Davis†

*Department of Chemistry, University of Arizona, Tucson, Arizona 85721; and †Department of Physics,
University of California, Berkeley, California 94720

Received March 8, 1996; in revised form May 10, 1996

The emission spectrum of FeF has been observed in the near infrared region from 9000 to 12 000 cm^{-1} . The bands were excited in a high temperature carbon tube furnace and recorded with a Fourier transform spectrometer at a resolution of 0.02 cm^{-1} . The observed bands have been assigned as the 0–1, 0–0, 1–0, and 2–0 bands of the $g^4\Delta_i - a^4\Delta_i$ transition analogous to the $F^4\Delta_i - X^4\Delta_i$ transition of FeH at 1 μm . Each vibrational band consists of four sub-bands assigned as $^4\Delta_{1/2} - ^4\Delta_{1/2}$, $^4\Delta_{3/2} - ^4\Delta_{3/2}$, $^4\Delta_{5/2} - ^4\Delta_{5/2}$, and $^4\Delta_{7/2} - ^4\Delta_{7/2}$. The rotational analysis of these bands has been performed and molecular constants have been determined. This work represents the first observation of the $g^4\Delta - a^4\Delta$ transition of FeF. We discuss the correspondence between the low-lying electronic states of FeF, FeH, and Fe^+ . © 1996 Academic Press, Inc.

INTRODUCTION

While the electronic spectra of many transition metal hydrides and oxides are relatively well characterized, only a few diatomic transition metal halides are known (1–17). The work on some of the transition metal halides has been summarized by Rosen (1) and by Jones and Krishnamurthy (2). For the 3d transition metal monofluorides high resolution analyses are available for ScF (3), CrF (4), MnF (5, 6), FeF (7, 8), CoF (9, 10), NiF (11), and CuF (12). The electronic spectra of most of the transition metal halides are very complex because of their high density of electronic states. Many of these states have high spin multiplicities and generally the spin components are well separated because of substantial spin–orbit interactions. The large spin–orbit coupling also promotes perturbations between nearby states, increasing the spectral complexity. In some cases, when the spin–orbit splittings become very large, the spectra begin to have a deceptively simple appearance again. In this case, however, it is difficult to determine the Hund's case (a) parentage of a transition without the analysis of many other bands in the spectrum as well as some theoretical guidance.

The electronic spectra of FeF have been observed previously in emission as well as in absorption. The early emission work on FeF was carried out using a hollow cathode lamp (1), flash photolysis (13), and chemiluminescence (14). Improved spectra were recorded by Pouilly *et al.* (7) using a King furnace and, particularly, a liquid-nitrogen-cooled composite-wall hollow cathode lamp. Pouilly *et al.* (7) carried out a rotational analysis of some of the bands in

the ultraviolet and, with some theoretical help (8), assigned the ground state as a $^6\Delta$ state. They concluded that the $X^6\Delta$ ground state is inverted so that the $^6\Delta_{9/2}$ spin component lies lowest in energy. Only bands connecting to the $^6\Delta_{9/2}$, $^6\Delta_{7/2}$, and $^6\Delta_{-1/2}$ spin components could be analyzed in their spectra. The *ab initio* calculations of Pouilly *et al.* (8) predicted the properties of several sextet and quartet electronic states and helped them assign the FeF bands observed in the ultraviolet region as belonging to $^6\Phi - X^6\Delta$ and $^6\Pi - X^6\Delta$ transitions (7). They also noticed (8) the strong similarity between the electronic structure of FeF and Fe^+ . Very recently the ground state of FeF has been confirmed as $X^6\Delta_i$ by the detection of pure rotational transitions in all six spin components (15). The only other published experimental datum available for FeF is the dissociation energy of 448 ± 21 kJ/mole (107 ± 5 kcal/mole) measured by high temperature mass spectrometry (16).

Experimental (17) and theoretical (18) studies of the iso-valent molecule, FeCl, are also available. Delaval and Schamps (18) found that the electronic structure of FeCl is very similar to that of FeF. Very recently the $X^6\Delta_{7/2}$ and $X^6\Delta_{5/2}$ spin components of the millimeter-wave spectrum of FeCl have been detected (19).

The discovery by radio astronomers (20, 21) of AlCl, KCl, NaCl, and AlF molecules in the circumstellar envelope of the carbon star IRC + 10216 is responsible for some of the recent spectroscopic interest in metal halides (15, 19). Iron-containing compounds are particularly favorable for astronomical detection in stellar atmospheres because of the relatively high (0.003%) cosmic abundance of iron. The ^{56}Fe nucleus is the most stable nucleus in terms of binding energy per nucleon and this enhances its cosmic abundance. FeH,

¹ Also, Department of Chemistry, University of Waterloo, Waterloo, Ontario, Canada N2L 3G1.

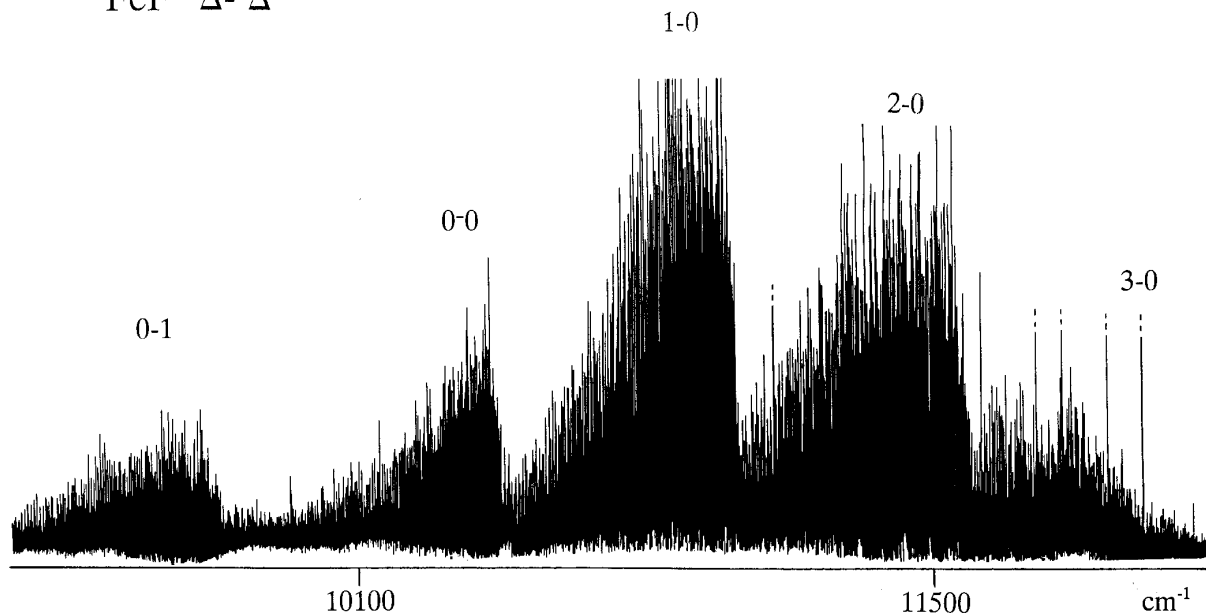
FeF $^4\Delta-^4\Delta$ 

FIG. 1. A compressed portion of the low resolution spectrum of the $g^4\Delta-a^4\Delta$ transition of FeF.

for example, has been identified in the spectra of sunspots and cool stars (22, 23).

High quality *ab initio* studies of most of the first row transition metal hydrides are available and generally good agreement has been observed between the available experimental data and the theoretical predictions. Unfortunately very few calculations are available for transition metal fluorides but the electronic structure is very similar to that of the corresponding hydrides. For example, our recent work on CoH (25) and CoF (26) demonstrates that these two molecules have almost identical electronic energy level patterns and that their red and infrared spectra are very similar.

Fortunately for our work on FeF, the FeH molecule has been studied in great detail in recent years (27–33). In the early theoretical studies (e.g., (27)), there was controversy over the nature of the ground electronic state because some calculations predicted a $^6\Delta_i$ ground state. The more recent calculations (28, 29) and experimental results (32, 33) prove that FeH has a $^4\Delta$ ground state. The $a^6\Delta_i$ state is very low-lying, however, and is located about 0.26 eV (2060 cm^{-1}) above the $X^4\Delta_i$ state (32).

Three FeH electronic transitions, $F^4\Delta-X^4\Delta$ (28, 30), $g^6\Phi-X^4\Delta$ (32), and $g^6\Phi-a^6\Delta$ (33), have been studied recently at high resolution. The $F^4\Delta-X^4\Delta$ transition of FeD has also been investigated in detail (34) near 1 μm . By analogy, a similar transition is expected for FeF in the same spectral region. In the present paper we report on the rotational analysis of the 0–1, 0–0, 1–0, and 2–0 bands of a new $g^4\Delta-a^4\Delta$ transition of FeF in the 9000–12 000 cm^{-1} region analogous to the $F^4\Delta-X^4\Delta$ transition of FeH.

EXPERIMENTAL

The near infrared bands of FeF were observed by the high temperature reaction of Fe atoms with CF_4 in a carbon tube furnace at about 2300°C. The initial experiment was intended to measure the infrared vibration–rotation bands of FeH formed by the reaction of Fe with H_2 . About 100 Torr of He was used as the buffer gas in all of the experiments. In

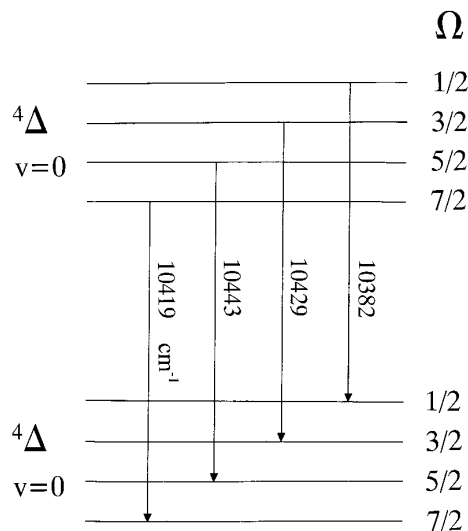


FIG. 2. A schematic energy level diagram of the $g^4\Delta-a^4\Delta$ transition of FeF with arrows marking the observed sub-bands. The sub-band origins for the 0–0 vibrational bands are listed.

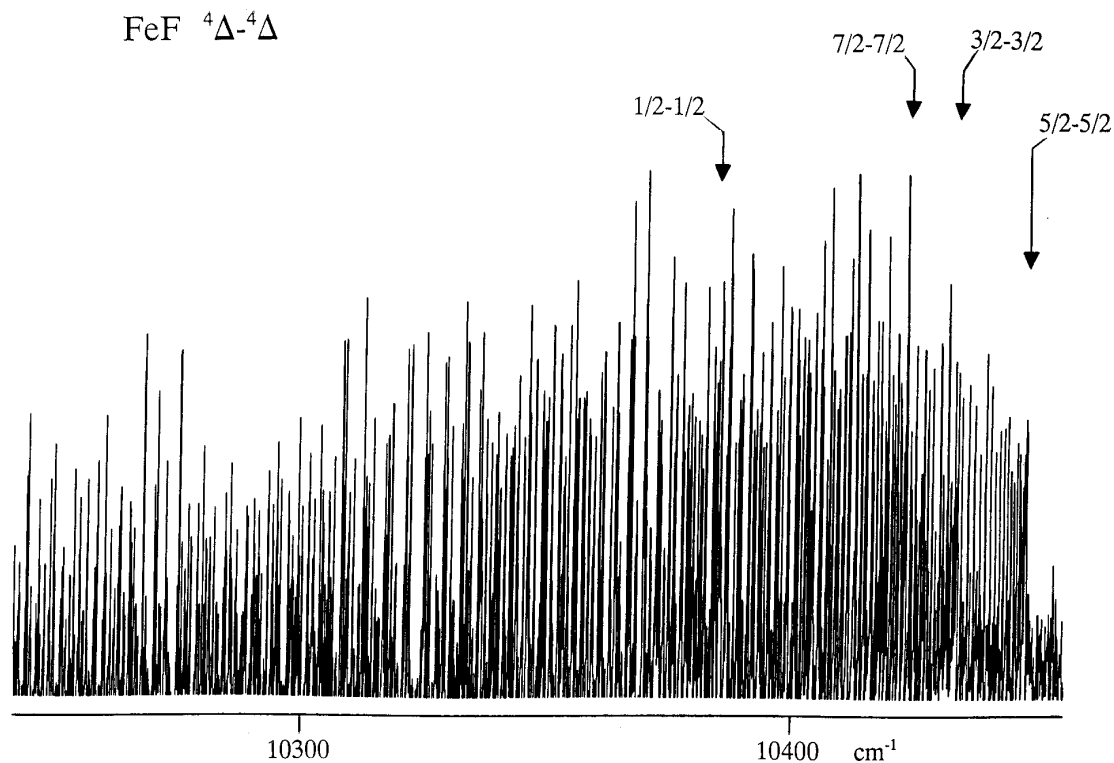


FIG. 3. A compressed portion of the 0-0 band of the $g^4\Delta\text{-}a^4\Delta$ system of FeF. The R -head positions of the different sub-bands have been marked by arrows.

this FeH experiment we first decided to monitor the $F^4\Delta\text{-}X^4\Delta$ transition near $1\ \mu\text{m}$ to make sure that we were making FeH and in order to maximize the FeH concentration. The $F^4\Delta\text{-}X^4\Delta$ bands had a signal-to-noise ratio of at least 30:1 but when we scanned in the $2000\text{-}4000\ \text{cm}^{-1}$ interval, we did not observe the predicted (35) vibration-rotation bands of FeH. In the end we decided to look for the FeF molecule in the near infrared region. We added a small amount of CF_4 instead of H_2 and, keeping the other experimental parameters the same, we observed strong FeF emission bands in the $9000\text{-}12\ 000\ \text{cm}^{-1}$ region.

The emission from the furnace was focused on to the 8 mm entrance aperture of the 1-m Fourier transform spectrometer of the National Solar Observatory at Kitt Peak. The spectra were recorded using silicon photodiode detectors and RG 850 filters at a resolution of $0.02\ \text{cm}^{-1}$. A total of four scans were co-added in about 25 min of integration; the spectra had a signal-to-noise ratio of about 15:1.

The spectral line positions were measured using a data reduction program called PC-DECOMP developed by J. Brault. The peak positions were determined by fitting a Voigt line shape function to each line. Since the molecules were excited in a carbon tube furnace, the observed spectra also contained impurity bands of the $A^2\Pi\text{-}X^2\Sigma^+$ transition of CN and some atomic lines. The FeF bands are not in the same spectral region as the CN bands so that we were not

troubled by presence of the CN impurity. In fact we have used the line positions of CN (36) to calibrate our spectrum. The molecular lines appear with a width of $0.07\ \text{cm}^{-1}$ and

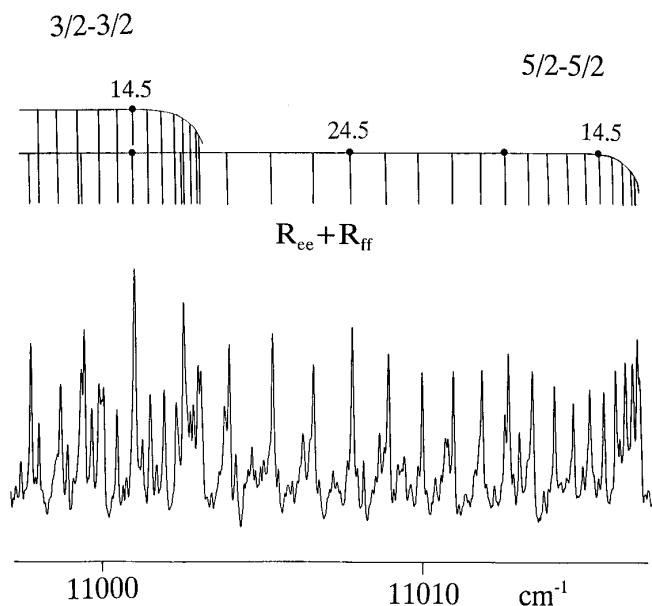


FIG. 4. An expanded portion of the 1-0 band of the $g^4\Delta_{5/2}\text{-}a^4\Delta_{5/2}$ sub-band near the R -head.

TABLE 1
Observed Line Positions (in cm^{-1}) for the $g^4\Delta_{1/2} - a^4\Delta_{1/2}$ Sub-band of FeF

J	1 - 0						2 - 0									
	Ree	O-C	Pee	O-C	Rff	O-C	Pff	O-C	Ree	O-C	Pee	O-C	Rff	O-C	Pff	O-C
9.5									11518.444	0						
10.5									11518.276	-2						
11.5																
12.5									11517.689	-6						
13.5																
14.5									11516.776	-2						
15.5									11516.202	8			11516.067	-10		
16.5									11515.533	6			11515.397	-5		
17.5			10926.713	-24					11514.785	9			11514.670	25		
18.5			10924.593	-6					11513.934	-7			11513.803	-0		
19.5			10922.380	-3					11513.023	-1			11512.870	-8		
20.5			10920.079	-12					11512.026	4						
21.5									11510.941	5						
22.5			10915.249	-24					11509.768	1			11509.584	-18		
23.5			10912.734	-16					11508.523	9	11474.746	-10				
24.5	10945.586	-9	10910.117	-30					11507.159	-18	11472.010	-9				
25.5	10944.330	2	10907.463	-5	10944.132	-8			11505.755	-1	11469.203	6				
26.5	10942.972	-10			10942.800	12			11504.259	7	11466.294	1				
27.5			10901.879	2	10941.369	12					11463.301	-5	11502.485	20		
28.5	10940.058	2	10898.950	-15	10939.866	18			11501.009	18	11460.226	-10	11500.798	12	11460.026	-7
29.5	10938.473	-4	10895.977	1	10938.272	11			11499.235	1	11457.083	2	11499.036	13		
30.5	10936.814	-4	10892.905	-5					11497.383	-11	11453.824	-20	11497.192	16	11453.639	10
31.5	10935.072	-9	10889.766	1	10934.862	9	10889.553	13	11495.481	11	11450.526	2	11495.250	4	11450.313	10
32.5	10933.266	0	10886.536	-8	10933.034	2	10886.315	3	11493.455	-5	11447.136	16	11493.227	-4	11446.903	10
33.5			10883.244	-1	10931.137	6	10883.016	10	11491.355	-12	11443.622	-12	11491.135	3	11443.406	6
34.5	10929.384	-16	10879.871	3	10929.160	7	10879.630	6	11489.189	-2	11440.081	17	11488.937	-12	11439.836	42
35.5	10927.347	-3	10876.422	8	10927.103	7	10876.161	-2			11436.404	-6	11486.685	4	11436.171	7
36.5	10925.237	16	10872.881	-2	10924.961	-1	10872.630	5	11484.593	9			11484.324	-6	11432.428	8
37.5	10923.014	0	10869.260	-13	10922.740	-7	10869.009	-1	11482.156	3			11481.879	-15	11428.574	-21
38.5	10920.723	-4	10865.570	-16	10920.458	3	10865.327	10	11479.649	11	11424.948	-1	11479.377	3	11424.696	10
39.5	10918.349	-14	10861.804	-18			10861.551	4	11477.048	8	11420.964	2	11476.768	-2	11420.685	-8
40.5	10915.909	-9			10915.631	-3	10857.709	10	11474.348	-9	11416.898	7	11474.087	7	11416.627	9
41.5	10913.395	-1	10854.059	-1	10913.107	1			11471.575	-13	11412.738	1	11471.302	-5	11412.463	4
42.5	10910.794	-0			10910.497	-2	10849.773	4	11468.741	5	11408.500	-0	11468.446	-3	11408.201	-15
43.5	10908.097	-17	10846.000	13	10907.821	9	10845.699	11	11465.796	-3	11404.173	-6	11465.481	-25	11403.870	-20
44.5	10905.348	-7	10841.836	2	10905.031	-16	10841.541	12	11462.772	-5	11399.788	13	11462.490	11	11399.464	-16
45.5	10902.522	4			10902.202	-0	10837.309	16	11459.667	-2	11395.289	1	11459.346	-21	11394.996	9
46.5	10899.610	10	10833.280	-15	10899.265	-15	10832.976	-2	11456.486	8			11456.137	-34		
47.5	10896.604	1	10828.910	2	10896.267	-11			11453.197	-5			11452.866	-24	11385.748	-2
48.5	10893.539	11	10824.457	13	10893.177	-19	10824.125	9	11449.838	-2	11381.340	17	11449.520	-3	11380.997	-10
49.5	10890.379	6	10819.912	11	10890.018	-17	10819.565	-4	11446.399	5			11446.031	-40*	11376.170	-10
50.5	10887.154	15	10815.289	8			10814.948	6	11442.878	16	11371.601	8			11371.239	-30
51.5	10883.838	13	10810.605	22			10810.230	-8	11439.254	8			11438.877	-37*		
52.5	10880.429	-4	10805.832	25			10805.445	-11	11435.560	16					11361.179	-18*
53.5			10800.968	16			10800.595	-2			11356.380	8				
54.5					10873.031	-11					11351.152	20	11427.437	-101*	11350.778	-11*
55.5	10869.756	-20	10790.986	-23			10790.645	2	11423.918	-9	11345.784	-23	11423.473	-104*	11345.381	-78*
56.5	10866.049	-15	10785.914	-6			10785.563	14	11419.881	-3			11419.441	-88*	11339.978	-68*
57.5	10862.259	-14	10780.746	-8			10780.386	10	11415.754	-2	11334.892	-12	11415.310	-86*	11334.480	-69*
58.5			10775.503	-5	10858.021	7	10775.125	-0	11411.545	3	11329.337	9	11411.077	-101*		
59.5	10854.441	-11	10770.186	2	10854.059	1	10769.797	0	11407.244	3	11323.661	-5	11406.671	-202*	11323.219	-83*
60.5	10850.417	-4			10850.027	6	10764.405	16	11402.863	7	11317.915	-6	11402.331	-152*	11317.462	-91*
61.5	10846.319	9	10759.296	-6	10845.892	-13	10758.911	8	11398.382	-3	11312.084	-7	11397.841	-167*	11311.633	-86*
62.5	10842.112	-7	10753.741	-2	10841.703	-6	10753.344	5	11393.827	0	11306.173	-6	11393.205	-241*	11305.676	-126*
63.5	10837.856	8			10837.450	19	10747.688	-9	11389.191	7	11300.179	-1			11299.623	-177*
64.5	10833.497	0	10742.377	-14	10833.083	9	10741.982	6	11384.449	-6	11294.106	7			11293.484	-230*
65.5	10829.069	4	10736.593	-4	10828.640	4	10736.182	6	11379.638	-2	11287.934	1			11287.206	-337*
66.5	10824.558	6	10730.710	-14			10730.302	5	11374.742	4	11281.680	-2				
67.5			10724.760	-12			10724.353	13	11369.749	-2	11275.360	13	11369.525	176*		
68.5			10718.738	-3	10814.847	6	10718.305	1	11364.674	-3	11268.918	-10	11364.380	109*	11268.689	162*
69.5			10712.631	-1	10810.082	2	10712.187	-3	11359.507	-10	11262.409	-14	11359.212	106*	11262.205	186*
70.5	10805.688	-10	10706.437	-7	10805.240	0	10705.988	-7			11255.850	15	11353.930	74*	11255.541	115*
71.5	10800.783	2	10700.179	2	10800.319	0	10699.712	-10	11348.926	-11	11249.161	-1	11348.585	67*	11248.832	83*
72.5	10795.793	8	10693.819	-12	10795.001	-15	10693.374	3			11242.412	8	11343.129	34*	11242.067	80*
73.5	10790.700	-7	10687.400	-7	10790.224	-8	10686.943	3	11338.008	-2	11235.553	-9	11337.619	35*	11235.175	35*
74.5	10785.563	14	10680.901	-1	10785.061	-6	10680.439	9			11228.635	1	11332.013	28	11228.220	11*

TABLE 1—Continued

J	1 - 0						2 - 0									
	Ree	O-C	Pee	O-C	Rff	O-C	Pff	O-C	Ree	O-C	Pee	O-C	Rff	O-C	Pff	O-C
75.5	10780.322	13	10674.318	-1	10779.828	7	10673.841	0	11326.722	-15	11221.631	9	11326.327	26	11221.226	34
76.5			10667.651	-5			10667.171	-1	11320.976	6	11214.534	9	11320.525	-5	11214.085	-6
77.5	10769.583	-3	10660.930	15	10769.096	12	10660.431	6	11315.117	1	11207.341	-2	11314.658	-12	11206.923	18
78.5	10764.104	3	10654.093	-1	10763.595	2	10653.596	-1	11309.188	14	11200.098	22	11308.727	2	11199.652	19
79.5	10758.546	10	10647.184	-9	10758.019	-2	10646.670	-19	11303.147	1	11192.712	-12	11302.695	4	11192.284	7
80.5	10752.912	22	10640.211	-2	10752.366	-1	10639.702	-1	11297.040	10	11185.274	-13	11296.577	6	11184.828	-6
81.5	10747.168	8	10633.151	-3	10746.632	1	10632.631	-6	11290.818	-9			11290.374	12	11177.314	7
82.5			10626.003	-13	10740.822	9	10625.491	0	11284.534	-2	11170.163	6	11284.076	9	11169.689	-6
83.5			10618.797	-0			10618.276	12	11278.167	9	11162.469	5	11277.680	-3	11161.993	-4
84.5	10729.477	-6	10611.501	3			10610.965	6	11271.691	-0	11154.670	-15	11271.215	3	11154.225	12
85.5	10723.421	-5	10604.122	2	10722.857	-9	10603.563	-10	11265.156	18	11146.829	8	11264.653	1	11146.338	-5
86.5			10596.671	9	10716.700	-19			11258.505	9	11138.858	-13	11258.003	-3	11138.388	-1
87.5	10711.077	11	10589.114	-10			10588.558	-3			11130.827	-9	11251.264	-6	11130.350	2
88.5	10704.761	-0	10581.504	-2	10704.171	-5	10580.927	-7	11244.950	2	11122.705	-9	11244.452	6	11122.199	-23
89.5			10573.817	9	10697.783	1	10573.236	8	11238.032	-10	11114.516	8	11237.524	-10	11114.004	-5
90.5	10691.916	10	10566.045	16	10691.312	9	10565.415	-25	11231.058	10	11106.208	-8	11230.548	15	11105.703	-7
91.5	10685.371	17	10558.184	14	10684.745	3	10557.566	-7	11223.995	30	11097.851	14	11223.456	12	11097.316	-10
92.5	10678.714	-6	10550.244	13	10678.097	-1	10549.616	-8	11216.787	-7			11216.266	0	11088.855	1
93.5			10542.207	-5	10671.373	3	10541.597	2					11208.978	-21	11080.297	0
94.5	10665.193	-9	10534.114	2	10664.554	-5	10533.486	1					11201.637	-6	11071.649	-4
95.5	10658.341	23	10525.933	2	10657.651	-14	10525.292	-2					11194.192	-6	11062.946	23
96.5	10651.342	-9	10517.663	-7	10650.682	-5									11054.111	5
97.5	10644.318	17													11045.210	8
98.5															11036.228	17

J	0 - 0						0 - 1									
	Ree	O-C	Pee	O-C	Rff	O-C	Pff	O-C	Ree	O-C	Pee	O-C	Rff	O-C	Pff	O-C
15.5					10384.660	-6										
16.5					10384.192	-3										
17.5	10383.773	-10			10383.658	5										
18.5	10383.173	-3			10383.036	-2										
19.5	10382.497	1	10353.897	13	10382.357	5										
20.5	10381.750	6	10351.708	3	10381.603	10										
21.5	10380.928	8	10349.458	3	10380.760	-2										
22.5	10380.025	1	10347.136	2	10379.853	-6	10346.975	6								
23.5	10379.053	-2	10344.737	-3			10344.573	3								
24.5			10342.272	-3	10377.836	-2	10342.104	6								
25.5	10376.892	-11	10339.745	6	10376.723	4	10339.568	13								
26.5	10375.713	-4			10375.527	1	10336.961	20			9654.826	16				
27.5	10374.456	-4	10334.446	-5	10374.262	-1	10334.263	8			9652.315	23				
28.5	10373.127	-3	10331.698	-3			10331.498	-0			9649.724	16				
29.5	10371.725	-3	10328.874	-4	10371.525	6	10328.670	1								
30.5	10370.269	16			10370.026	-12	10325.769	1								
31.5	10368.720	13	10323.003	-14	10368.487	2	10322.787	-10								
32.5	10367.089	3	10319.972	-7	10366.858	-2	10319.752	-1								
33.5	10365.385	-10	10316.877	7	10365.156	-6	10316.636	-2	9684.311	-16			9684.056	17	9635.506	-10
34.5	10363.616	-14	10313.689	-0	10363.395	4	10313.461	9	9682.745	-20			9682.474	5	9632.546	16
35.5	10361.781	-11	10310.437	1	10361.546	-2	10310.192	-1			9629.792	12	9680.838	5	9629.462	-17
36.5	10359.878	-3	10307.105	-7	10359.621	-11	10306.864	1			9626.661	-9	9679.130	-0		
37.5	10357.917	18			10357.636	-8	10303.463	2			9623.481	-12	9677.369	9	9623.191	13
38.5	10355.839	-3	10300.247	-1	10355.578	-4	10299.980	-8	9675.832	-14					9619.939	10
39.5	10353.725	11	10296.717	10	10353.437	-10	10296.440	-3			9616.944	1	9673.625	5	9616.634	20
40.5	10351.531	19	10293.099	4	10351.237	-4	10292.822	-3	9671.975	-10	9613.563	-6	9671.662	12	9613.237	3
41.5	10349.255	18	10289.413	1	10348.947	-14	10289.134	-3			9610.128	1	9669.619	8	9609.795	7
42.5	10346.903	13	10285.662	6	10346.612	4	10285.366	-10			9606.625	4				
43.5			10281.838	10	10344.168	-15	10281.531	-12	9665.681	-8			9665.323	-13		
44.5	10341.981	6	10277.934	5	10341.678	-5	10277.635	-5	9663.448	-8	9599.420	9			9599.050	-2
45.5	10339.413	6	10273.966	9	10339.093	-18	10273.661	-2	9661.153	-3	9595.701	-5	9660.775	-15	9595.347	6
46.5	10336.777	10	10269.924	10			10269.608	-7	9658.782	-6	9591.937	2	9658.396	-20	9591.553	-11
47.5	10334.060	7	10265.798	-0	10333.724	-24*	10265.481	-13	9656.347	-6	9588.078	-20			9587.721	-0
48.5	10331.271	5	10261.597	-14	10330.928	-28*	10261.285	-17	9653.848	-2	9584.216	21	9653.455	-11	9583.799	-14
49.5	10328.404	-1	10257.354	4	10328.069	-22*	10257.021	-17*	9651.286	7	9580.217	-8	9650.863	-26	9579.817	-21
50.5					10325.098	-54*	10252.682	-21*	9648.636	-5	9576.192	3	9648.254	8	9575.786	-10

TABLE 1—Continued

J	0 - 0						0 - 1									
	Ree	O-C	Pee	O-C	Rff	O-C	Pff	O-C	Ree	O-C	Pee	O-C	Rff	O-C	Pff	O-C
51.5	10322.472	10	10248.622	8	10322.085	-55*	10248.305	11*	9645.946	10	9572.090	2	9645.506	-28	9571.666	-22
52.5							10243.795	-19*	9643.171	10	9567.914	-5	9642.731	-24*		
53.5			10239.585	-4			10239.229	-32*			9563.679	-5	9639.852	-56*	9563.257	-17
54.5									9637.414	3	9559.385	3	9636.978	-16*	9558.942	-26*
55.5							10229.887	-51*	9634.441	8	9555.007	-8	9633.971	-40*		
56.5	10306.303	-14	10225.514	5	10305.902	-73*	10225.101	-68*	9631.389	1	9550.585	5	9630.913	-47*	9550.113	-41*
57.5	10302.865	-1	10220.656	-15	10302.461	-59*	10220.270	-58*	9628.273	-1			9627.787	-55*		
58.5	10299.347	6	10215.746	-14	10298.922	-69*	10215.355	-57*	9625.096	3	9541.514	2	9624.661	7*	9541.026	-50*
59.5	10295.741	-1	10210.756	-20	10295.316	-73*	10210.351	-75*	9621.844	1	9536.877	-1	9621.341	-57*	9536.396	-40*
60.5	10292.067	-2	10205.708	-13	10291.628	-84*	10205.291	-75*	9618.525	-1	9532.181	4	9618.004	-71*	9531.668	-62*
61.5	10288.322	1	10200.606	14	10287.867	-94*	10200.154	-81*			9527.412	2	9614.589	-95*	9526.899	-58*
62.5	10284.487	-13	10195.401	10	10284.027	-108*	10194.921	-109*	9611.670	-14	9522.570	-6	9611.128	-95*	9522.045	-73*
63.5	10280.600	-3	10190.108	-9	10280.110	-126*	10189.637	-116*	9608.161	1	9517.685	9	9607.565	-129*	9517.117	-95*
64.5	10276.634	2	10184.777	6	10276.125	-137*	10184.284	-119*	9604.576	8	9512.712	5			9512.137	-102*
65.5	10272.580	-7	10179.353	2	10272.010	-203*	10178.822	-159*	9600.918	10	9507.676	3			9507.103	-95*
66.5	10268.449	-18	10173.862	3	10267.908	-181*	10173.340	-144*	9597.190	11	9502.571	-1	9596.479	-216*	9501.974	-117*
67.5	10264.273	2	10168.293	-0	10263.644	-247*	10167.764	-152*	9593.368	-13	9497.398	-5	9592.669	-223*	9496.766	-151*
68.5	10260.004	2	10162.657	2	10259.333	-285*	10162.101	-174*			9492.165	-3	9588.680	-338*	9491.502	-173*
69.5	10255.644	-14	10156.962	18	10254.889	-381*	10156.321	-239*	9585.576	-3	9486.864	-1	9584.628	-448*	9486.176	-191*
70.5	10251.246	9	10151.158	-2	10250.314	-533*	10150.443	-330*	9581.568	-6	9481.503	7	9580.525	-540*	9480.659	-332*
71.5	10246.741	-2	10145.303	1	10246.818	469*	10144.535	-377*	9577.491	-9	9476.066	6			9475.118	-430*
72.5	10242.180	8	10139.386	14	10242.079	304*	10138.405	-573*	9573.366	9	9470.559	4			9469.496	-541*
73.5	10237.529	1	10133.370	3	10237.355	228*	10133.428	457*	9569.141	-4	9464.989	5			9464.935	475*
74.5	10232.798	-9	10127.282	-7	10232.574	171*	10127.213	323*	9564.866	2	9459.348	2	9564.521	194*	9459.135	321*
75.5	10228.011	0	10121.141	3	10227.728	124*	10120.971	235*	9560.517	4	9453.635	-5	9560.095	126*	9453.321	219*
76.5			10114.901	-13	10222.841	112*	10114.679	171*	9556.100	8	9447.862	-6	9555.634	92*	9447.485	164*
77.5			10108.623	7			10108.292	85*	9551.613	10	9442.011	-17	9551.109	65*	9441.591	118*
78.5	10213.163	-5	10102.253	8	10212.823	71*	10101.936	103*			9436.117	-2	9546.532	55*	9435.649	92*
79.5	10208.057	-13	10095.803	3	10207.696	47*	10095.441	56*			9430.146	2			9429.644	72*
80.5	10202.902	6	10089.286	5	10202.506	34*	10088.931	69*	9537.700	-15	9424.108	7	9537.175	44*	9423.578	57*
81.5	10197.643	-2	10082.689	0	10197.252	35*	10082.322	57*	9532.944	-2	9417.981	-9	9532.484	31*	9417.462	61*
82.5	10192.314	-3	10076.007	-14	10191.928	41*	10075.644	49*	9528.105	-3			9527.536	31*	9411.259	46*
83.5	10186.915	0	10069.289	8	10186.490	10	10068.888	36*	9523.205	6	9405.544	-22	9522.570	-16	9404.989	32*
84.5	10181.426	-9	10062.470	4	10181.006	10	10062.060	27*					9517.612	15	9398.662	29*
85.5	10175.879	-0	10055.588	10			10055.143	2	9513.175	4	9392.870	-0	9512.552	15	9392.261	21
86.5			10048.614	-1			10048.180	6	9508.064	12	9386.413	-7	9507.407	1	9385.787	8
87.5	10164.542	5	10041.578	1	10164.091	4	10041.125	-7	9502.850	-13	9379.900	-2	9502.210	5	9379.268	18
88.5	10158.748	-4			10158.298	1			9497.596	-7	9373.319	2				
89.5	10152.899	10	10027.287	7	10152.434	4	10026.842	16	9492.269	-4	9366.657	-6			9366.003	18
90.5	10146.956	7	10020.012	-8			10019.559	-2			9359.929	-12			9359.260	11
91.5			10012.685	1			10012.209	-12	9481.400	1	9353.149	-1			9352.453	8
92.5	10134.845	6	10005.277	2	10134.365	-0	10004.807	0	9475.852	-5	9346.294	2			9345.560	-12
93.5	10128.667	-1			10128.181	-8	9997.319	-2	9470.242	-1	9339.354	-12			9338.627	-3
94.5	10122.403	-16	9990.229	-2					9464.546	-13	9332.383	13			9324.525	-14
95.5	10116.077	-16					9982.112	-1	9458.805	1	9325.315	8			9324.525	-14
96.5	10109.673	-17	9974.883	-4	10109.195	2	9974.407	10	9452.999	22	9318.203	29			9317.381	-7
97.5	10103.203	-5			10102.706	1	9966.609	2	9447.079	0					9310.171	2
98.5	10096.631	-17							9441.131	21					9302.890	9
99.5			9951.310	2											9295.515	-7
100.5			9943.299	2												
101.5																
102.5															9280.593	-3
103.5			9918.803	-9											9273.012	-16
104.5															9265.392	1
105.5			9902.127	17											9257.676	-7
106.5			9893.646	2											9249.919	15
107.5			9885.117	13											9242.063	7
108.5			9876.487	1												
109.5			9867.793	1												
110.5			9859.028	6												
111.5			9850.163	-12												
112.5			9841.252	1												
113.5			9832.235	-16												
114.5																
115.5			9814.034	14												
116.5			9804.782	-6												
117.5			9795.482	2												

TABLE 2
Observed Line Positions (in cm⁻¹) for the $g^4\Delta_{3/2} - d^4\Delta_{3/2}$ Sub-band of FeF

J	1 - 0								2 - 0							
	Ree	O-C	Pee	O-C	Rff	O-C	Pff	O-C	Ree	O-C	Pee	O-C	Rff	O-C	Pff	O-C
6.5			10993.031	312*			10993.031	319*								
7.5			10991.770	332*			10991.770	339*								
8.5			10990.406	323*			10990.406	331*								
9.5			10989.008	357*			10989.008	366*								
10.5	11003.070	342*	10987.484	339*	11003.070	352*	10987.484	350*	11566.909	321*			11566.909	331*		
11.5	11002.925	365*	10985.914	353*	11002.925	376*	10985.914	364*	11566.684	336*			11566.684	347*		
12.5	11002.721	406*	10984.264	364*	11002.721	417*	10984.264	376*	11566.398	373*			11566.398	384*		
13.5	11002.384	390*	10982.548	384*	11002.384	402*	10982.548	396*	11566.016	396*			11566.016	408*		
14.5	11002.009	413*	10980.764	412*	11002.009	426*	10980.764	425*	11565.566	433*			11565.566	445*		
15.5	11001.579	457*	10978.900	437*	11001.579	470*	10978.900	450*	11565.029	465*			11565.029	479*		
16.5	11001.104	533*	10977.016	517*	11001.104	547*	10977.016	531*	11564.426	513*			11564.426	527*		
17.5	11000.538	595*	10975.070	612*	11000.538	610*	10975.070	626*	11563.774	596*			11563.774	610*		
18.5	10999.987	747*	10973.102	761*	10999.987	762*	10973.102	775*	11563.096	735*			11563.096	749*		
19.5	10999.437	979*	10971.141	992*	10999.437	994*	10971.141	1008*	11562.447	984*			11562.447	999*		
20.5																
21.5	10995.791	-875*	10964.676	-857*	10995.791	-860*	10964.676	-842*								
22.5	10995.074	-582*	10962.574	-538*	10995.074	-566*	10962.574	-522*	11557.724	-547*			11557.724	-531*		
23.5	10994.207	-360*	10960.236	-378*	10994.207	-344*	10960.236	-362*	11556.686	-356*			11556.686	-341*		
24.5	10993.143	-260*	10957.787	-253*	10993.143	-244*	10957.787	-237*	11555.474	-256*			11555.474	-240*		
25.5	10991.975	-186*	10955.191	-198*	10991.975	-170*	10955.191	-182*	11554.148	-188*			11554.148	-172*		
26.5	10990.700	-142*	10952.525	-138*	10990.700	-127*	10952.525	-122*	11552.684	-175*	11514.863	-127*	11552.684	-159*		
27.5	10989.336	-111*	10949.754	-106*	10989.336	-96*	10949.754	-91*	11551.208	-91*	11511.928	-107*	11551.208	-76*	11511.928	-94*
28.5	10987.899	-75*	10946.894	-86*	10987.899	-60*	10946.894	-72*	11549.582	-75*	11508.959	-39*	11549.582	-60*	11508.919	-67*
29.5	10986.345	-79*	10943.962	-63*	10986.345	-65*	10943.962	-49*	11547.867	-64*	11505.825	-53*	11547.867	-50*	11505.825	-41*
30.5	10984.741	-55*	10940.941	-52*	10984.741	-41*	10940.941	-38*	11546.073	-50*	11502.648	-28*	11546.073	-36*	11502.648	-17*
31.5	10983.029	-64*	10937.848	-36*	10983.029	-51*	10937.848	-23*	11544.195	-37*	11499.350	-42*	11544.195	-24*	11499.350	-31*
32.5	10981.269	-42*	10934.671	-28*	10981.269	-29*	10934.671	-16*	11542.228	-29*	11495.977	-49*	11542.228	-17*	11495.977	-38*
33.5	10979.435	-17*	10931.396	-43*	10979.435	-5	10931.396	-31*	11540.158	-42*	11492.564	-14	11540.158	-31*	11492.554	-14*
34.5	10977.502	-14*	10928.075	-26*	10977.502	-3	10928.075	-16	11538.049	-11	11489.045	-2	11538.049	0	11489.045	8
35.5	10975.494	-9	10924.681	-6	10975.494	1	10924.681	3			11485.426	-9			11485.426	1
36.5			10921.189	-7			10921.189	1	11533.526	-4	11481.734	-7	11533.526	4	11481.734	2
37.5	10971.238	-5	10917.628	-1	10971.238	2	10917.628	6	11531.146	6	11477.962	-1	11531.146	13	11477.962	6
38.5	10968.997	-0	10913.989	3	10968.997	5	10913.989	9	11528.667	1	11474.087	-16	11528.667	7	11474.087	-11
37.5							10910.282	21	11526.102	-8	11470.154	-8	11526.102	-4	11470.154	-4
40.5	10964.274	2	10906.469	0	10964.274	5	10906.469	3	11523.481	11	11466.148	10	11523.481	13	11466.148	12
41.5	10961.808	15	10902.604	9	10961.808	16	10902.604	9	11520.745	-1	11462.037	6	11520.745	-0	11462.037	7
42.5	10959.234	-2	10898.639	-6	10959.234	-3	10898.639	-7	11517.937	-2	11457.846	3	11517.937	-3	11457.846	2
43.5	10956.604	3	10894.622	4	10956.604	0	10894.622	1	11515.056	7	11453.564	-8	11515.056	5	11453.564	-11
44.5	10953.905	16	10890.518	4	10953.905	11	10890.518	-1	11512.064	-11	11449.225	7	11512.064	-16	11449.225	2
45.5	10951.101	3	10886.315	-19	10951.101	-4			11509.033	16			11509.033	9		
46.5	10948.235	5	10882.077	0	10948.235	-4	10882.077	-9	11505.893	17	11440.273	10	11505.893	8	11440.273	1
47.5	10945.286	3			10945.286	-9			11502.648	-3	11435.669	7	11502.648	-14	11435.669	-5
48.5	10942.266	8	10873.341	9	10942.266	-6	10873.341	-5	11499.350	8	11430.989	11	11499.350	-6	11430.989	-3
49.5	10939.170	15			10939.170	-2	10868.868	7					11495.977	12		
50.5	10935.982	8	10864.290	10	10935.982	-11	10864.290	-9	11492.470	-2			11492.470	-21		
51.5	10932.712	-2	10859.653	15	10932.712	-24	10859.653	-7			11416.446	15	11488.937	5	11416.446	-7
52.5	10929.384	8	10854.932	13	10929.384	-17	10854.932	-12	11485.283	19	11411.426	10	11485.283	-6	11411.426	-15
53.5	10925.961	2	10850.141	17	10925.961	-26	10850.141	-11	11481.556	20	11406.321	2	11481.556	-8	11406.347	-0
54.5	10922.471	6	10845.253	3	10922.471	-25	10845.253	-6			11401.138	-1			11401.169	-1
55.5	10918.881	-10	10840.290	-10			10840.335	0	11473.826	2	11395.873	-3	11473.846	-12		
56.5	10915.249	11	10835.267	-6	10915.249	-27	10835.305	-6	11469.860	18			11469.877	-2		
57.5	10911.522	15	10830.158	-10	10911.522	-26	10830.202	-7	11465.796	21			11465.807	-9		
58.5	10907.715	18	10824.987	0	10907.715	-27	10825.025	-6	11461.625	1	11379.589	-0			11379.633	-1
59.5			10819.724	-4	10903.836	-21	10819.769	-7	11457.374	-14	11374.000	5	11457.443	7		
60.5	10899.830	-10	10814.399	8			10814.429	-14			11368.314	-3	11453.111	-9	11368.367	-2
61.5	10895.784	-10	10808.968	-10	10895.861	12	10809.026	-7	11448.663	0	11362.555	-1	11448.710	-8	11362.608	-5
62.5	10891.653	-15	10803.475	-11	10891.736	8	10803.534	-12	11444.161	-11			11444.233	1		
63.5	10887.447	-17	10797.917	-0	10887.527	0	10797.982	1	11439.596	-2	11350.778	-8	11439.669	8		
64.5	10883.166	-13	10792.282	11	10883.244	-3	10792.330	-10	11434.941	3	11344.780	5	11435.009	3	11344.840	-4
65.5	10878.807	-8	10786.578	30	10878.889	2	10786.611	-8	11430.186	-8	11338.674	-8	11430.279	13	11338.755	1
66.5	10874.362	-10	10780.746	-0	10874.451	2	10780.816	-7	11425.365	1	11332.511	6	11425.454	13	11332.571	-11
67.5	10869.839	-11	10774.859	-8	10869.927	-4	10774.948	1	11420.441	-8	11326.237	-8	11420.530	-0	11326.327	1
68.5	10865.244	-5	10768.893	-17	10865.327	-7	10769.001	6	11415.438	-11	11319.896	-6	11415.540	6	11319.970	-17
69.5	10860.566	-1	10762.898	22			10762.974	9	11410.346	-18	11313.481	6	11410.456	2	11313.561	4
70.5	10855.802	-4	10756.761	-3	10855.909	9			11405.188	-5	11306.962	-2	11405.306	18		
71.5	10850.958	-7	10750.574	0	10851.081	17	10750.673	0	11399.921	-17	11300.376	5	11400.040	3	11300.470	0
72.5	10846.048	4	10744.304	-2	10846.157	9	10744.421	12	11394.621	24	11293.699	5	11394.718	18	11293.790	-7
73.5	10841.045	1	10737.965	6	10841.157	5	10738.080	12			11286.949	16			11287.054	14

TABLE 2—Continued

1 - 0									2 - 0							
J	Ree	O-C	Pee	O-C	Rff	O-C	Pff	O-C	Ree	O-C	Pee	O-C	Rff	O-C	Pff	O-C
74.5			10731.549	13	10836.091	14	10731.654	5			11280.087	-1	11383.791	21	11280.220	19
75.5	10830.812	9	10725.043	10	10830.943	23	10725.171	19			11273.175	15	11378.214	36	11273.315	38
76.5	10825.580	17	10718.485	31			10718.597	20			11266.169	21	11372.532	34	11266.315	44
77.5			10711.847	51			10711.982	58			11259.011	-41	11366.794	60	11259.237	57
78.5	10814.847	6	10705.022	-38							11251.811	-62				
79.5			10698.190	-55	10809.415	-82	10698.300	-82			11244.567	-43			11244.693	-54
80.5	10803.774	-24	10691.312	-41	10803.887	-53	10691.451	-44			11237.248	-15			11237.367	-38
81.5	10798.123	-33	10684.373	-8	10798.289	-14	10684.519	-10			11229.826	-6			11229.939	-40
82.5	10792.418	-15	10677.328	-4	10792.585	0	10677.472	-12			11222.321	4			11222.456	-13
83.5	10786.578	-52	10670.212	7	10786.773	-14									11214.852	-23
84.5	10780.746	-0			10780.905	-4	10663.150	-11			11207.055	19			11207.202	5
85.5	10774.777	-5	10655.717	2			10655.886	5			11199.274	6				
86.5	10768.757	21	10648.354	3	10768.893	-14	10648.516	-7			11191.451	34			11191.600	11
87.5	10762.606	-4	10640.898	-12			10641.083	-4			11183.525	44				
88.5	10756.397	-6	10633.380	-10	10756.588	4	10633.570	-1			11175.508	46			11175.642	-1
89.5	10750.117	2	10625.799	8							11167.393	34			11167.526	-18
90.5	10743.780	34	10618.135	21	10743.941	6									11159.339	-22
91.5			10610.382	25	10737.511	21	10610.559	6								
92.5			10602.551	28	10730.947	-15	10602.717	-6							11142.750	9
93.5			10594.645	36	10724.353	-1	10594.794	-19							11134.295	-9
94.5			10586.661	44			10586.833	8							11125.777	-5
95.5			10578.584	38			10578.765	8							11117.173	-4
96.5					10704.043	4										
97.5							10562.379	-7								
98.5					10690.094	6	10554.075	-6								
99.5					10683.007	18	10545.686	-12								
100.5					10675.811	3	10537.237	2								
101.5					10668.553	7	10528.689	-4								
102.5							10520.060	-11								
103.5							10511.368	-2								

0 - 0									0 - 1							
J	Ree	O-C	Pee	O-C	Rff	O-C	Pff	O-C	Ree	O-C	Pee	O-C	Rff	O-C	Pff	O-C
11.5	10433.077	283*			10433.077	294*			9749.020	-10			9749.020	-5		
12.5	10433.001	373*			10433.001	385*			9748.918	-18			9748.918	-13		
13.5	10432.789	398*	10412.797	399*	10432.789	411*	10412.797	411*	9748.754	-23			9748.754	-18		
14.5	10432.508	425*	10411.096	431*	10432.508	438*	10411.096	444*	9748.542	-12			9748.542	-6		
15.5	10432.170	466*	10409.314	454*	10432.170	479*	10409.314	467*	9748.261	-5						
16.5	10431.778	523*	10407.515	529*	10431.778	537*	10407.515	543*	9747.902	-10			9747.902	-3		
17.5	10431.336	601*	10405.611	570*	10431.336	615*	10405.611	584*	9747.483	-10			9747.483	-3		
18.5	10430.886	742*	10403.771	745*	10430.886	757*	10403.771	760*	9747.003	-7			9747.003	0		
19.5	10430.465	983*	10401.893	954*	10430.465	998*	10401.839	968*	9746.457	-4			9746.457	3		
20.5									9745.841	-6	9715.877	-5	9745.841	1	9715.877	2
21.5	10427.080	-865*	10395.683	-874*	10427.080	-850*	10395.683	-859*	9745.169	1	9713.787	7	9745.169	8	9713.787	14
22.5	10426.520	-551*	10393.717	-544*	10426.520	-535*	10393.717	-528*	9744.416	-9	9711.613	-2	9744.416	-2	9711.613	6
23.5	10425.764	-361*	10391.520	-373*	10425.764	-345*	10391.520	-357*	9743.616	0	9709.384	1	9743.616	7	9709.384	8
24.5	10424.848	-260*	10389.205	-251*	10424.848	-245*	10389.205	-235*	9742.728	-12	9707.086	-1	9742.728	-5	9707.086	5
25.5	10423.827	-193*	10386.751	-196*	10423.827	-177*	10386.751	-180*	9741.810	9	9704.709	-19	9741.810	16	9704.709	-13
26.5	10422.699	-162*	10384.224	-144*	10422.699	-146*	10384.224	-129*	9740.797	2	9702.313	10	9740.797	8	9702.313	17
27.5	10421.516	-115*	10381.603	-117*	10421.516	-100*	10381.603	-101*	9739.725	0	9699.814	-0	9739.725	6	9699.814	6
28.5	10420.253	-76*	10378.910	-90*	10420.253	-61*	10378.910	-75*			9697.261	1			9697.261	7
29.5	10418.906	-50*	10376.149	-61*	10418.906	-35*	10376.149	-46*	9737.386	-2	9694.641	0	9737.386	4	9694.641	5
30.5	10417.468	-44*	10373.309	-39*	10417.468	-30*	10373.309	-26*	9736.110	-11	9691.961	3	9736.110	-6	9691.961	8
31.5	10415.956	-40*	10370.380	-37*	10415.956	-27*	10370.380	-24*	9734.801	12	9689.210	1	9734.801	17	9689.210	5
32.5	10414.376	-33*	10367.385	-30*	10414.376	-20*	10367.385	-17*	9733.370	-20	9686.395	-1	9733.370	-16	9686.395	3
33.5	10412.735	-15	10364.328	-14	10412.735	-3	10364.328	-2	9731.932	6	9683.524	6	9731.932	8	9683.524	9
34.5	10411.003	-16	10361.184	-15	10411.003	-6	10361.184	-4	9730.389	-7	9680.565	-10	9730.389	-5	9680.565	-8
35.5	10409.213	-5	10357.997	12	10409.213	4	10357.997	22	9728.793	-8	9677.570	2	9728.793	-7	9677.570	4
36.5			10354.698	-2			10354.698	6	9727.131	-8	9674.504	9	9727.131	-8	9674.504	9
37.5	10405.391	-8	10351.339	-5	10405.391	-1	10351.339	2	9725.412	0	9671.365	7	9725.412	-1	9671.365	6
38.5	10403.375	-7	10347.915	-3	10403.375	-1	10347.915	3	9723.629	10	9668.159	3	9723.629	8	9668.159	1
39.5	10401.295	2	10344.415	-6	10401.295	7	10344.415	-2	9721.776	16	9664.885	-3	9721.776	13	9664.905	13
40.5	10399.140	8	10340.858	5	10399.140	11	10340.858	8	9719.849	15	9661.567	10	9719.849	10	9661.567	6
41.5	10396.899	0	10337.220	6	10396.899	1	10337.220	7			9658.165	6			9658.165	0
42.5	10394.592	-2			10394.592	-3			9715.793	8	9654.714	17	9715.793	0	9654.714	10

TABLE 2—Continued

J	0 - 0								0 - 1							
	Ree	O-C	Pe	O-C	Rff	O-C	Pff	O-C	Ree	O-C	Pe	O-C	Rff	O-C	Pff	O-C
43.5	10392.224	7	10329.727	3	10392.224	4	10329.727	0	9713.664	3	9651.176	7	9713.664	-6	9651.176	-2
44.5	10389.777	9	10325.884	11	10389.777	4	10325.884	7	9711.467	-5	9647.565	-11	9711.467	-15	9647.565	-22
45.5	10387.258	11	10321.969	19	10387.258	4	10321.969	12	9709.221	6	9643.916	-2	9709.221	-6	9643.916	-14
46.5	10384.660	7	10317.949	-7	10384.660	-2	10317.949	-16	9706.899	7	9640.202	7	9706.899	-7	9640.202	-7
47.5	10381.995	7	10313.894	2	10381.995	4	10313.894	-9	9704.511	8	9636.420	13	9704.511	-8	9636.420	-3
48.5	10379.240	-9	10309.763	7	10379.240	-23	10309.763	-6	9702.055	9	9632.542	-12	9702.055	-10		
49.5	10376.444	6	10305.543	-6	10376.444	-11	10305.543	-22	9699.525	1			9699.525	-20	9628.651	-4
50.5	10373.563	8	10301.265	-5	10373.563	-11	10301.265	-24	9696.946	11			9696.946	-12	9624.669	-4
51.5	10370.610	11	10296.920	-1	10370.610	-11	10296.920	-23			9620.609	9	9694.307	3	9620.609	-17
52.5			10292.507	7	10367.605	10	10292.507	-18	9691.549	-7	9616.492	7	9691.549	-34	9616.492	-21
53.5	10364.476	7	10288.005	-3	10364.476	-21	10288.005	-31	9688.758	-8	9612.304	-1	9688.758	-38*	9612.304	-31*
54.5	10361.299	4	10283.428	-17	10361.299	-27	10283.428	-48			9608.050	-8	9685.869	-74*	9608.050	-41*
55.5	10358.063	15	10278.811	1	10358.063	-20	10278.811	-33			9603.733	-14			9603.721	-62*
56.5	10354.698	-31	10274.104	0	10354.698	-68	10274.104	-37	9679.984	-11	9599.377	7	9679.984	-50*	9599.377	-32*
57.5	10351.339	4	10269.309	-17	10351.339	-37	10269.309	-58	9676.948	11	9594.926	-1	9676.948	-31*	9594.926	-43*
58.5	10347.856	-13	10264.477	-0	10347.856	-58	10264.477	-45	9673.806	-5	9590.429	11	9673.806	-51*	9590.429	-35*
59.5	10344.314	-17	10259.540	-16	10344.314	-65	10259.600	-4	9670.625	6	9585.861	17	9670.625	-43*	9585.860	-33*
60.5	10340.707	-11	10254.557	-7	10340.707	-63	10254.619	3	9667.402	43*	9581.229	25	9667.399	-13*	9581.229	-28*
61.5	10337.018	-15	10249.491	-9	10337.018	-70	10249.554	-1	9664.059	28*	9576.505	7	9664.063	-25*	9576.618	64*
62.5	10333.262	-12	10244.351	-13	10333.262	-72	10244.425	1	9660.702	65*	9567.018	13			9571.861	75*
63.5	10329.399	-43	10239.147	-9	10329.500	-6	10239.229	9	9657.232	58*	9567.018	129*			9567.106	153*
64.5	10325.505	-31	10233.860	-17	10325.592	-11	10233.931	-14					9653.636	-77*	9561.819	-235*
65.5	10321.551	-5	10228.520	-6	10321.627	-2	10228.592	-6			9556.803	-212*	9650.076	-43*	9556.934	-155*
66.5	10317.493	-10	10223.111	8	10317.583	4	10223.172	-8			9551.936	-44*	9646.348	-110*	9551.936	-122*
67.5	10313.393	16	10217.600	-8	10313.461	4	10217.684	-4			9546.793	-85*			9546.891	-70*
68.5	10309.165	-11			10309.265	4	10212.123	-3	9638.786	-60*	9541.652	-58*	9638.885	-47*	9541.732	-65*
69.5	10304.902	1	10206.402	-0	10304.980	-11	10206.500	8	9634.917	-58*			9635.036	-32*	9536.526	-43*
70.5	10300.550	-3	10200.695	4	10300.661	14	10200.783	-2	9630.988	-50*	9531.132	-45*	9631.112	-24*	9531.247	-27*
71.5	10296.149	19	10194.921	13			10195.019	13	9626.987	-46*	9525.763	-47*	9627.114	-21*	9525.888	-25*
72.5	10291.628	-6	10189.056	4	10291.736	-1	10189.153	-3	9622.919	-40*	9520.352	-25*	9623.057	-11	9520.461	-25
73.5	10287.065	2	10183.115	-10			10183.229	-4	9618.784	-32*	9514.848	-31*	9618.927	-4	9514.984	-8
74.5	10282.421	3	10177.127	2	10282.546	15	10177.245	7	9614.589	-17	9509.296	-17	9614.718	-8	9509.422	-11
75.5	10277.712	14	10171.062	9	10277.834	17	10171.182	12	9610.299	-28	9503.670	-12	9610.443	-10	9503.799	-9
76.5	10272.908	3	10164.934	26	10273.046	19	10165.060	29	9605.965	-14	9497.974	-9	9606.124	12	9498.114	-1
77.5	10268.072	35	10158.631	-61	10268.215	51	10158.859	40			9492.209	-10	9601.704	2	9492.358	1
78.5			10152.337	-65			10152.487	-48	9597.067	-12	9486.390	3			9486.539	7
79.5			10145.980	-60	10258.151	-62			9592.521	-4	9480.477	-12	9592.673	-5		
80.5			10139.573	-33	10253.102	-25	10139.707	-41	9587.887	-16	9474.522	-2	9588.078	15	9474.675	-9
81.5			10133.074	-25	10247.946	-19	10133.230	-16			9468.501	8	9583.390	11	9468.649	-11
82.5			10126.511	-8	10242.715	-12	10126.653	-18	9578.442	-10	9462.391	-5	9578.636	10	9462.574	4
83.5			10119.849	-17	10237.413	-3	10120.014	-9	9573.622	-1	9456.235	4	9573.799	-6	9456.412	-0
84.5			10113.138	-4	10232.018	-11	10113.285	-18	9568.711	-14	9450.002	4			9450.194	5
85.5			10106.345	1	10226.561	-6	10106.518	8	9563.758	-0	9443.700	-0			9443.892	-7
86.5			10099.466	-7	10221.043	13	10099.646	2	9558.720	-2	9437.346	10			9437.554	11
87.5			10092.527	-2	10215.429	11	10092.705	-0	9553.599	-17	9430.908	5			9431.103	-16
88.5			10085.503	-9	10209.725	-5	10085.691	-2	9548.437	-4	9424.407	3			9424.636	7
89.5			10078.422	-1	10203.962	-5	10078.597	-12							9418.079	8
90.5					10198.124	-5	10071.469	18			9411.210	5	9538.143	18	9411.455	8
91.5					10192.214	-0	10064.230	10			9404.517	12	9532.764	12	9404.763	6
92.5			10056.709	-8	10186.234	9	10056.923	7					9527.323	14	9398.014	14
93.5			10049.336	2	10180.168	8	10049.542	4			9390.913	10			9391.185	10
94.5			10041.878	-2	10174.022	4					9384.004	2			9384.297	12
95.5			10034.364	12	10167.783	-18	10034.572	9			9377.042	9	9510.565	1	9377.323	-3
96.5			10026.740	-10	10161.484	-24	10026.970	5			9370.005	8	9504.842	-1	9370.298	-3
97.5			10019.069	-6	10155.137	-1	10019.300	6			9362.884	-10	9499.040	-13	9363.189	-20
98.5					10148.680	-13	10011.546	-4							9493.200	8
99.5											9348.475	-10				
100.5													9481.237	-27	9341.526	-5
101.5													9475.175	-20		

a maximum signal-to-noise ratio of about 15:1, so that the line positions are expected to be accurate to about ± 0.005 cm^{-1} . However, since there is considerable overlapping and

blending caused by the presence of different sub-bands in the same region, the measurement error is often somewhat higher for blended and weak lines.

TABLE 3
Observed Line Positions (in cm⁻¹) for the $g^4\Delta_{5/2} - g^4\Delta_{5/2}$ Sub-band of FeF

J	0 - 1				0 - 0				1 - 0				2 - 0				
	Ree+Rff	O-C	Pee+Pff	O-C	Ree+Rff	O-C	Pee+Pff	O-C	Ree+Rff	O-C	Pee+Pff	O-C	Ree+Rff	O-C	Pee+Pff	O-C	
3.5												11010.211	-1				
4.5												11009.165	-2				
5.5							10438.216	-13				11008.040	-10				
6.5							10437.054	-13				11006.853	-4				
7.5							10435.831	-6				11005.581	-8				
8.5							10434.519	-18				11004.240	-6		11567.973	5	
9.5							10433.166	-2	11016.971	4		11002.828	-2		11566.509	6	
10.5							10431.733	2	11016.894	5		11001.329	-8	11580.390	6	11564.947	-10
11.5						10447.342	17					10999.756	-15	11580.154	-4	11563.325	-6
12.5	9763.819	-6			10447.171	-2	10428.641	-8	11016.507	2		10998.122	-8	11579.855	2	11561.621	-3
13.5			9743.721	-5	10446.944	-8	10427.003	-1	11016.198	-3		10996.408	-6	11579.467	-0	11559.836	-2
14.5	9763.467	8	9742.087	-2	10446.659	-3	10425.285	-6	11015.818	-4		10994.619	-4	11578.999	-2	11557.971	-0
15.5	9763.198	18	9740.404	17	10446.301	-1	10423.508	-0	11015.374	7		10992.752	-6	11578.436	-17	11556.018	-6
16.5	9762.876	39*	9738.683	61*	10445.868	-5	10421.652	-5	11014.838	-1		10990.816	-1	11577.821	-4	11553.985	-11
17.5	9762.493	63*	9736.849	56*	10445.373	-1	10419.758	21	11014.233	-1		10988.805	2	11577.104	-11	11551.888	-0
18.5	9762.042	83*	9734.981	80*	10444.803	-3	10417.745	-3	11013.547	-8		10986.714	1	11576.327	1	11549.697	-3
19.5	9761.529	105*	9733.045	100*	10444.168	-0	10415.691	2	11012.803	3		10984.543	-7	11575.454	-1	11547.423	-8
20.5	9760.960	135*	9731.052	126*	10443.462	1	10413.551	-11	11011.969	-1		10982.314	3	11574.498	-5	11545.098	16
21.5	9760.318	156*	9729.000	157*	10442.694	9	10411.353	-12	11011.066	2		10979.992	-5	11573.466	-4	11542.650	-2
22.5	9759.620	185*	9726.888	191*	10441.829	-9	10409.102	2	11010.084	0		10977.610	1	11572.363	7	11540.158	16
23.5	9758.869	226*	9724.749	263*	10440.928	6	10406.761	-5	11009.023	-4		10975.144	-2	11571.162	-0	11537.551	-1
24.5	9758.051	263*	9722.465	252*	10439.945	9	10404.375	13	11007.902	6		10972.605	-3	11569.866	-21	11534.885	4
25.5	9757.176	307*	9720.166	289*	10438.889	7	10401.893	3	11006.692	3		10970.017	21	11568.531	2	11532.122	-8
26.5	9756.242	357*	9717.824	347*	10437.762	6	10399.350	1	11005.417	10		10967.307	-1	11567.088	-4	11529.301	3
27.5	9755.252	414*	9715.394	380*	10436.568	6	10396.743	5	11004.052	3		10964.552	6	11565.566	-7	11526.377	-9
28.5	9754.213	487*	9712.969	482*	10435.307	9	10394.069	10	11002.627	10		10961.715	7	11563.964	-8	11523.370	-24
29.5	9753.129	578*	9710.457	560*	10433.983	20	10391.332	22	11001.104	-3		10958.792	-5	11562.292	1	11520.334	13
30.5	9751.985	674*	9707.908	665*	10432.583	24	10388.494	2	10999.535	12		10955.809	-2	11560.531	3	11517.165	-1
31.5	9750.819	812*	9705.332	805*	10431.107	22	10385.616	11	10997.874	10		10952.755	7	11558.691	7	11513.934	2
32.5	9749.626	987*	9702.728	981*	10429.568	27	10382.687	38	10996.150	23		10949.625	12	11556.766	7	11510.618	1
33.5	9748.464	1257*	9700.152	1248*	10427.954	27	10379.631	8	10994.334	18		10946.404	3	11554.762	10	11507.236	13
34.5	9747.352	1641*	9697.619	1622*	10426.271	29*	10376.556	27*	10992.445	16*		10943.126	10	11552.674	11	11503.749	2
35.5	9746.394	2244*	9695.267	2240*	10424.515	27*	10373.390	25*	10990.482	17*		10939.769	15	11550.506	12	11500.197	7
36.5					10422.699	35*	10370.165	33*	10988.453	27*		10936.337	19	11548.268	26	11496.561	8
37.5	9738.683	-2155*	9684.735	-2164*	10420.803	34*	10366.858	28*	10986.344	33*		10932.828	21	11545.924	15	11492.843	8
38.5	9737.526	-1559*	9682.169	-1571*	10418.848	43*	10363.492	33*	10984.148	27*		10929.245	24	11543.512	18	11489.045	8
39.5			9679.336	-1182*	10416.810	40*	10360.056	37*	10981.887	33*		10925.583	22	11541.014	16	11485.160	3
40.5	9734.469	-918*	9676.312	-919*	10414.717	53*	10356.538	29*	10979.541	30*		10921.847	22*	11538.450	30*	11481.208	10*
41.5	9732.710	-732*	9673.139	-744*	10412.539	51*	10352.973	44*	10977.130	38*		10918.058	44*	11535.796	37*	11477.185	28*
42.5	9730.823	-610*	9669.862	-610*	10410.293	51*	10349.325	45*	10974.635	38*		10914.161	34*	11533.056	38*	11473.065	29*
43.5	9728.868	-491*	9666.506	-491*	10407.976	52*	10345.605	42*	10972.066	41*		10910.210	44*	11530.227	33*	11468.863	29*
44.5	9726.801	-420*	9663.035	-424*	10405.606	69*	10341.826	51*	10969.429	52*		10906.173	43*	11527.328	40*	11464.572	21*
45.5	9724.668	-351*	9659.490	-367*	10403.146	67*	10337.981	63*	10966.688	35*		10902.070	52*	11524.335	34*	11460.226	39*
46.5	9722.465	-287*	9655.887	-307*	10400.631	81*	10334.060	68*	10963.918	65*		10897.892	60*	11521.291	61*	11455.780	37*
47.5	9720.166	-255*	9652.205	-261*	10398.023	72*	10330.073	77*	10961.048	72*		10893.622	52*	11518.138	60*	11451.261	45*
48.5	9717.824	-202*	9648.459	-217*	10395.357	76*	10326.006	76*	10958.103	81*		10889.310	78*	11514.919	75*	11446.679	69*
49.5	9715.394	-172*	9644.637	-184*	10392.643	104*	10321.903	108*	10955.088	95*		10884.913	93*	11511.603	75*	11441.994	71*
50.5	9712.889	-153*	9640.749	-155*	10389.858	131*	10317.710	120*	10952.003	117*		10880.429	97*	11508.223	94*	11437.250	96*
51.5	9710.329	-124*	9636.788	-136*	10386.997	152*	10313.461	145*	10948.835	133*		10875.899	130*	11504.777	129*	11432.428	124*
52.5	9707.692	-107*	9632.772	-109*	10384.087	196*	10309.165	193*	10945.626	184*		10871.298	168*	11501.247	163*	11427.538	165*
53.5	9704.996	-86*	9628.677	-98*	10381.114	249*	10304.775	217*	10942.357	252*		10866.654	238*	11497.680	242*	11422.602	241*
54.5	9702.215	-84*	9624.532	-73*					10939.082	390*		10862.005	379*	11494.087	378*	11417.619	351*
55.5	9699.395	-56*	9620.313	-58*												11412.605	511*
56.5	9696.496	-43*	9616.027	-48*													
57.5	9693.531	-31*	9611.682	-33*					10927.538	-449*		10846.334	-471*				
58.5	9690.498	-22*	9607.264	-28*	10364.416	-254*	10281.174	-269*	10923.991	-275*		10841.436	-277*			11395.773	-311*
59.5	9687.401	-12	9602.793	-13	10361.033	-184*	10276.416	-194*	10920.271	-195*		10836.351	-194*	11473.624	-201*	11390.379	-205*
60.5	9684.203	-8	9598.250	-5	10357.557	-136*	10271.558	-148*	10916.442	-148*		10831.148	-154*	11469.433	-166*	11384.849	-155*
61.5	9681.001	-2	9593.637	-4	10353.986	-109*	10266.623	-111*	10912.512	-124*		10825.859	-124*	11465.161	-130*	11379.220	-122*
62.5	9677.698	-2	9588.960	-4	10350.326	-102*	10261.597	-94*	10908.499	-105*		10820.481	-107*	11460.784	-115*	11373.475	-122*
63.5	9674.338	5	9584.216	-7	10346.612	-75*	10256.494	-83*	10904.412	-83*		10815.025	-92*	11456.334	-91*	11367.689	-83*
64.5	9670.908	9	9579.427	10	10342.805	-70*	10251.329	-65*	10900.225	-83*		10809.495	-75*	11451.790	-77*	11361.786	-80*
65.5	9667.399	-1	9574.554	6	10338.927	-64*	10246.079	-61*	10895.977	-67*		10803.888	-59*	11447.136	-90*	11355.795	-82*
66.5	9663.844	9	9569.624	8	10334.981	-54*	10240.784	-32*	10891.653	-49*		10798.186	-63*	11442.438	-64*	11349.732	-75*
67.5	9660.212	7	9564.624	5	10330.939	-68*	10235.369	-52*	10887.241	-41*		10792.418	-56*	11437.632	-61*	11343.596	-59*

TABLE 3—Continued

J	0-1				0-0				1-0				2-0			
	Ree+Rff	O-C	Pee+Pff	O-C	Ree+Rff	O-C	Pee+Pff	O-C	Ree+Rff	O-C	Pee+Pff	O-C	Ree+Rff	O-C	Pee+Pff	O-C
68.5	9656.515	7	9559.563	5	10326.867	-40*	10229.929	-27*	10882.745	-40*	10786.578	-45*	11432.749	-53*	11337.358	-64*
69.5	9652.753	7	9554.442	10	10322.712	-22*	10224.393	-28*	10878.177	-33*	10780.656	-40*	11427.790	-37*	11331.061	-46*
70.5	9648.922	5	9549.247	5	10318.462	-28*	10218.789	-26*	10873.512	-44*	10774.651	-43*	11422.731	-38*	11324.660	-50*
71.5	9645.023	2	9543.989	1	10314.152	-19*	10213.121	-18*	10868.796	-28*	10768.580	-34*			11318.190	-41*
72.5	9641.057	-2	9538.663	-6	10309.763	-19*	10207.358	-34*	10863.988	-26*	10762.427	-31*	11412.373	-27*	11311.646	-24*
73.5	9637.035	4	9533.282	-4	10305.300	-19*	10201.552	-22*	10859.102	-23*	10756.196	-30*	11407.067	-23*	11305.003	-25*
74.5	9632.933	-3	9527.834	-3	10300.766	-18	10195.671	-14	10854.146	-13	10749.907	-10	11401.672	-25	11298.283	-20
75.5	9628.767	-6	9522.318	-5	10296.172	-3	10189.714	-11	10849.089	-24	10743.522	-10	11396.202	-17	11291.498	1
76.5	9624.532	-12	9516.742	-3	10291.488	-7	10183.688	-7	10843.975	-15	10737.057	-14	11390.647	-10	11284.590	-18
77.5	9620.241	-6	9511.094	-6	10286.733	-7	10177.578	-16	10838.779	-9	10730.521	-11	11385.018	7	11277.636	-1
78.5	9615.875	-8	9505.380	-11	10281.910	-3	10171.419	-3	10833.499	-10	10723.917	-0			11270.577	-7
79.5	9611.439	-10	9499.614	-2	10277.000	-13	10165.165	-13	10828.123	-23	10717.219	-6			11263.428	-21
80.5	9606.955	6	9493.778	4			10158.859	-4	10822.705	-3	10710.459	2	11367.554	-13	11256.220	-11
81.5	9602.400	19	9487.878	12	10266.994	2	10152.487	9	10817.192	2	10703.612	0	11361.577	-7	11248.935	4
82.5	9597.789	46*			10261.866	-5	10146.028	7	10811.580	-13	10696.691	2			11241.546	-3
83.5	9593.163	126*	9475.843	-9	10256.674	-3	10139.496	4	10805.921	3	10689.688	-3	11349.376	12	11234.086	2
84.5					10251.415	5	10132.880	-12	10800.163	1	10682.615	1	11343.129	1	11226.538	0
85.5							10126.225	4	10794.326	-1	10675.472	12	11336.813	7	11218.912	5
86.5	9578.358	-146*	9457.189	-140*	10240.664	12	10119.483	5	10788.411	-2	10668.241	10	11330.377	-22	11211.206	11
87.5	9573.425	-95*	9450.915	-104*	10235.160	-3	10112.670	6	10782.421	2	10660.930	7	11323.926	18	11203.410	10
88.5	9568.383	-83*	9444.570	-73*	10229.607	7	10105.784	7	10776.355	9	10653.559	22			11195.519	-5
89.5	9563.269	-72*	9438.143	-54*	10223.978	15	10098.831	12	10770.186	-7	10646.086	11				
90.5	9558.075	-71*	9431.651	-34*	10218.262	12	10091.809	20	10763.978	18	10638.549	15	11303.932	8		
91.5	9552.857	-23*	9425.081	-22*	10212.469	5	10084.691	4	10757.660	13	10630.940	22				
92.5	9547.516	-26*	9418.459	8*	10206.621	17	10077.525	12	10751.285	30	10623.257	35			11163.200	14
93.5	9542.132	-0*	9411.765	35*			10070.278	12	10744.820	39	10615.494	45				
94.5			9404.998	58*	10194.663	6	10062.951	3			10607.670	71				
95.5			9398.166	86*									11268.918	3	11138.052	-12
96.5			9391.274	125*			10048.067	-27			10591.632	-32	11261.663	7	11129.504	-19
97.5			9384.299	152*	10176.157	-20	10040.546	-12			10583.571	-9	11254.318	5	11120.895	-5
98.5			9377.279	205*			10032.931	-19			10575.420	3	11246.888	5		
99.5			9370.180	251*	10163.465	-16	10025.267	-2			10567.189	12	11239.385	17	11103.390	-15
100.5			9363.031	319*	10157.017	-3	10017.508	-8			10558.850	-9	11231.750	-17		
101.5					10150.492	9					10550.461	-1	11224.077	-3		
102.5					10143.861	-10	10001.789	-1			10541.995	9				
103.5					10137.177	-6					10533.444	11			11067.409	-5
104.5					10130.398	-20	9985.772	0			10524.799	-1			11058.204	-4
105.5					10123.583	5	9977.660	7							11048.927	8
106.5					10116.663	2	9969.470	9			10507.300	0			11039.538	-8
107.5					10109.673	4	9961.190	-5			10498.433	2				
108.5							9952.844	-12			10489.487	3				
109.5											10480.452	-6				
110.5							9935.959	2			10471.342	-11				
111.5											10462.165	-3				
112.5											10452.904	-1				

OBSERVATIONS AND ANALYSIS

According to Pouilly *et al.* (8) the ground state of FeF correlates with the $3d^6 4s^2$ (a^5D) atomic limit of Fe and arises from the electronic configuration $3d_{Fe}^6(\sigma\pi^2\delta^3)4s\sigma_{Fe}2p_F^6(\sigma^2\pi^4)$, which can also be labeled as $8\sigma^2 3\pi^4 9\sigma 4\pi^2 1\delta^3 10\sigma$. This configuration results in numerous electronic states of which the ${}^6\Delta$ state is calculated to be the lowest in energy. Among the quartet states, the ${}^4\Delta$ state from the same configuration is lowest in energy and is predicted to lie at about 8000 cm^{-1} above the ground state (8). These *ab initio* calcu-

lations are relatively crude and it is more useful to use the very extensive calculations of FeH by Langhoff and Bauschlicher (28) as a guide (see discussion below).

The new bands of FeF are located in the 9000 to 12 000 cm^{-1} spectral region. The observed spectra consist of five groups of bands with *R*-heads at 9764, 10 447, 11 017, 11 580, and 12 140 cm^{-1} . These bands have been assigned as 0-1, 0-0, 1-0, 2-0, and 3-0, vibrational bands, respectively. The next bands (1-2, 1-1, 2-1, 3-1, and 4-1) in the $\Delta v = -1, 0, 1, 2,$ and 3 sequences could not be identified because of their weaker intensity and overlapping from the

TABLE 4
Observed Line Positions (in cm⁻¹) for the $g^4\Delta_{7/2} - d^4\Delta_{7/2}$ Sub-band of FeF

J	0 - 1		0 - 0		1 - 0		2 - 0	
	Ree+Rff O-C	Pee+Pff O-C	Ree+Rff O-C	Pee+Pff O-C	Ree+Rff O-C	Pee+Pff O-C	Ree+Rff O-C	Pee+Pff O-C
6.5						10980.351	12	
7.5						10979.101	13	
8.5				10409.870	1	10977.765	1	
9.5		9724.588 -14		10408.534	13	10976.375	8	
10.5		9723.235 -11						
11.5					10990.287 -2	10973.367	10	11551.888 -4
12.5		9720.347 -4	10422.561 -5	10404.075 -1	10990.091 7	10971.748 6	11551.610 -1	11533.416 1
13.5		9718.797 -16	10422.364 -7	10402.461 2	10989.811 5	10970.055 1	11551.251 -0	11531.658 1
14.5	9738.540 -3	9717.205 -7	10422.108 0	10400.775 -2	10989.466 11	10968.296 1	11550.819 7	11529.829 8
15.5	9738.306 5	9715.544 -6	10421.775 -4	10399.032 5	10989.031 -0	10966.465 3	11550.303 8	11527.908 1
16.5	9737.994 -4		10421.388 7	10397.219 10	10988.544 10	10964.552 -5	11549.697 -2	11525.906 -8
17.5	9737.627 -6	9712.041 -1	10420.917 1		10987.976 12	10962.574 -4	11549.026 2	11523.847 5
18.5	9737.201 -4	9710.189 -7	10420.370 -14	10393.372 -2	10987.324 4	10960.523 -5	11548.268 -2	11521.697 4
19.5	9736.711 -5	9708.282 -6	10419.786 2		10986.607 3	10958.406 2	11547.423 -15	11519.465 -0
20.5	9736.163 -2	9706.319 -1	10419.111 -6	10389.277 5	10985.816 2	10956.205 -3	11546.513 -13	11517.165 7
21.5	9735.554 2	9704.292 2	10418.371 -11	10387.122 2	10984.947 -4		11545.540 4	11514.785 11
22.5	9734.888 10	9702.215 16	10417.578 -2	10384.898 -2	10984.016 2	10951.584 -14	11544.469 2	11512.305 -6
23.5	9734.148 7	9700.049 2	10416.710 2	10382.628 13		10949.181 -2	11543.318 -1	11509.768 -1
24.5		9697.839 7	10415.776 6	10380.258 -3		10946.713 17	11542.091 -0	11507.159 10
25.5	9732.482 0	9695.566 9	10414.773 8	10377.836 -5	10980.764 1	10944.132 -3	11540.784 -1	11504.450 -1
26.5	9731.571 12	9693.228 7	10413.689 -3	10375.368 15	10979.541 8	10941.508 5	11539.396 -4	11501.675 2
27.5	9730.589 16*	9690.841 19*	10412.539 -11	10372.798 -1	10978.217 -13	10938.790 -6	11537.941 7	11498.816 -2
28.5	9729.547 20*	9688.375 13*		10370.165 -11	10976.849 -3		11536.393 2	11495.868 -16
29.5	9728.441 24*	9685.869 28*	10410.057 -7	10367.497 10	10975.401 0	10933.164 -3	11534.765 -3	11493.463 -28
30.5	9727.273 28*	9683.285 27*	10408.711 -7	10364.724 -7	10973.872 -5	10930.232 -10	11533.056 -10	11489.775 -6
31.5	9726.039 28*	9680.643 30*	10407.311 6	10361.900 -7	10972.269 -9	10927.242 -3	11531.281 -3	11486.614 3
32.5	9724.749 34*	9677.943 35*	10405.819 -4	10359.008 -8	10970.604 -2	10924.168 -7	11529.423 1	11483.361 -2
33.5	9723.395 39*	9675.159 18*	10404.275 1	10356.047 -11	10968.849 -11	10921.024 -7	11527.474 -8	11480.037 1
34.5	9721.984 49*	9672.356 45*	10402.655 -1	10353.039 6	10967.039 -1	10917.807 -8	11525.451 -10	11476.627 -4
35.5	9720.499 48*	9669.472 52*	10400.959 -11	10349.935 -5	10965.140 -6	10914.520 -5	11523.370 8	11473.155 8
36.5	9718.961 57*	9666.506 38*	10399.223 7	10346.780 1	10963.175 -4	10911.160 -4	11521.180 -2	11469.593 9
37.5	9717.355 60*	9663.508 54*	10397.385 -8	10343.544 -8	10961.139 3	10907.715 -13	11518.919 -4	11465.946 3
38.5	9715.692 69*	9660.448 70*	10395.509 7	10340.254 -3	10959.017 -3	10904.216 -3	11516.582 -2	11462.229 5
39.5	9713.967 79*	9657.303 63*	10393.545 4	10336.901 7	10956.820 -10	10900.623 -14	11514.156 -10	11458.418 -6
40.5	9712.177 86*	9654.118 77*	10391.520 7	10333.476 12	10954.563 -3	10896.976 -6	11511.667 -1	11454.556 10
41.5	9710.329 98*	9650.874 94*	10389.429 13	10329.975 9	10952.227 -0	10893.250 -4	11509.090 1	11450.580 -10
42.5	9708.419 112*	9647.565 108*	10387.258 7	10326.411 10	10949.815 1	10889.449 -4	11506.439 8	11446.542 -12
43.5	9706.444 123*	9644.184 112*	10385.042 25*	10322.787 20	10947.324 -3	10885.573 -6	11503.691 -2	11442.438 -3
44.5	9704.414 142*	9640.749 124*	10382.749 35*	10319.070 3	10944.764 -1	10881.622 -8	11500.874 -0	11438.244 -3
45.5	9702.313 154*	9637.259 142*	10380.384 43*	10315.315 17*	10942.124 -4	10877.598 -11	11497.968 -8	11433.973 -1
46.5	9700.152 168*	9633.706 161*		10311.496 34*	10939.414 -3	10873.512 -2	11494.995 -2	11429.627 4
47.5	9697.931 187*	9630.098 185*	10375.474 84*	10307.607 49*	10936.628 -4	10869.347 2	11491.936 -3	11425.182 -11
48.5	9695.566 124*	9626.342 125*	10372.913 102*	10303.646 60*	10933.774 2	10865.101 -2	11488.800 1	11420.685 2
49.5	9693.227 151*	9622.624 163*	10370.278 116*	10299.620 74*	10930.831 -5	10860.796 8	11485.579 -0	11416.083 -12
50.5	9690.786 139*	9618.786 144*	10367.385 -60*	10295.525 86*	10927.826 0	10856.384 -15	11482.291 11	11411.426 -1
51.5	9688.313 159*	9614.879 120*	10364.605 -53*	10291.388 125*	10924.751 10	10851.941 5	11478.907 8	11406.671 -9
52.5	9685.771 173*		10361.737 -65*	10286.953 -66*	10921.585 4	10847.408 8	11475.444 6	11401.854 0
53.5	9683.189 211*	9607.023 213*	10358.815 -61*	10282.657 -50*	10918.349 3	10842.800 9	11471.905 9	11396.958 10
54.5	9680.569 274*	9603.030 289*	10355.839 -41*	10278.255 -72*	10915.034 -1	10838.120 13	11468.273 0	11391.975 12
55.5	9677.879 332*		10352.770 -45*	10273.820 -59*	10911.661 11	10833.358 9	11464.572 3	11386.914 15
56.5			10349.642 -38*	10269.309 -53*	10908.199 10	10828.532 15	11460.784 -1	11381.766 11
57.5			10346.437 -38*	10264.728 -50*	10904.665 13	10823.624 11	11456.919 0	11376.533 2
58.5			10343.168 -34*	10260.091 -33*	10901.052 11	10818.637 4		11371.239 11
59.5			10339.834 -23*	10255.363 -40*	10897.357 4	10813.590 10	11448.958 13	11365.856 10
60.5			10336.419 -23*	10250.590 -23*		10808.464 12	11444.817 -20	11360.401 17
61.5			10332.939 -19*	10245.732 -22*	10889.766 15	10803.268 18	11440.672 26*	11354.868 26*
62.5	9655.435 -1085*		10329.399 -4	10240.784 -43*	10885.849 12	10797.995 21	11436.404 29*	11349.235 14*
63.5	9652.530 -728*	9562.575 -736*	10325.769 -8	10235.811 -20*	10881.869 23	10792.635 11	11432.048 27*	11343.545 26*
64.5	9649.390 -543*	9558.075 -541*	10322.085 3	10230.763 -3	10877.783 3*	10787.231 31*	11427.623 36*	11337.765 27*
65.5	9646.116 -426*	9553.430 -429*	10318.318 2	10225.628 -4	10873.678 40*	10781.733 32*	11423.100 29*	11331.908 32*
66.5	9642.732 -355*	9548.684 -354*	10314.489 10	10220.433 3	10869.459 40*	10776.172 44*	11418.514 41*	11325.983 48*
67.5	9639.273 -294*	9543.856 -298*	10310.587 15*	10215.176 17*	10865.196 72*	10770.536 56*	11413.844 51*	11319.970 56*
68.5	9635.732 -251*	9538.953 -254*	10306.617 23*	10209.847 29*		10764.821 63*	11409.090 59*	11313.868 56*
69.5	9632.116 -218*	9533.979 -218*	10302.588 44*	10204.444 36*		10759.037 76*	11404.261 73*	11307.703 73*
70.5	9628.425 -193*	9528.932 -192*	10298.483 59*	10199.000 70*	10851.876 95*	10753.187 97*	11399.370 108*	11301.467 99*
71.5	9624.669 -169*	9523.818 -170*	10294.329 95*	10193.487 105*	10847.312 132*	10747.278 135*	11394.381 127*	11295.161 135*
72.5	9620.847 -146*	9518.638 -149*	10290.134 163*	10187.930 164*	10842.707 205*	10741.323 202*	11389.362 198*	11288.800 197*
73.5	9616.947 -136*	9513.396 -129*				10735.420 394*	11384.379 387*	11282.480 380*

TABLE 4—Continued

J	0 - 1		0 - 0		1 - 0		2 - 0	
	Rec+Rff O-C	Pec+Pff O-C	Rec+Rff O-C	Pec+Pff O-C	Rec+Rff O-C	Pec+Pff O-C	Rec+Rff O-C	Pec+Pff O-C
74.5	9612.988	-119*	9508.071	-127*				
75.5	9608.966	-100*	9502.704	-103*				
76.5	9604.867	-92*	9497.262	-91*	10170.149	-349*	10827.688	-321*
77.5	9600.709	-77*	9491.760	-76*	10164.393	-211*	10822.844	-180*
78.5	9596.482	-66*	9486.174	-80*	10176.113	-175*	10716.113	-175*
79.5	9592.185	-58*	9480.551	-58*	10827.791	-188*	11367.791	-188*
80.5	9587.821	-51*	9474.838	-62*	10267.440	-150*	10158.492	-148*
81.5	9583.889	-47*	9469.081	-45*	10262.775	-124*	10152.487	-119*
82.5	9578.897	-37*	9463.258	-31*	10258.036	-100*	10146.403	-98*
83.5	9574.335	-30*	9457.363	-26*	10243.347	-67*	10127.714	-56*
84.5	9569.703	-27*	9451.399	-24*	10238.302	-61*	10121.328	-59*
85.5	9565.012	-16*	9445.378	-16*	10233.194	-45*	10114.901	-31*
86.5	9560.247	-12	9439.291	-9	10228.011	-32*	10108.360	-49*
87.5	9555.415	-9	9433.135	-6	10222.733	-40*	10101.790	-24*
88.5	9550.531	9	9426.918	-1	10217.400	-32*	10095.117	-32*
89.5	9545.563	10	9420.639	8	10211.998	-20*	10088.375	-38*
90.5	9540.520	2	9414.296	16	10206.500	-30*	10081.582	-25*
91.5	9535.431	16*	9407.880	17*	10200.942	-27*	10074.713	-17*
92.5	9530.260	14*	9401.398	16*	10195.319	-17	10067.773	-10
93.5	9525.030	22*	9394.879	43*	10189.637	9	10060.752	-13
94.5	9519.726	22*	9388.260	36*	10183.837	-11	10053.659	-16
95.5	9514.373	42*	9381.598	50*	10177.990	-4	10046.506	-10
96.5	9508.960	69*	9374.869	62*	10172.063	-4	10039.276	-8
97.5	9503.489	105*	9368.117	116*	10166.061	-4	10031.982	1
98.5					10159.989	-1	10024.610	3
99.5			9354.092	-101*	10153.848	6	10017.162	-0
100.5			9347.156	-35*	10147.620	2	10009.664	18
101.5			9340.099	-24*	10141.320	-0	10002.061	4
102.5			9332.985	-5	10134.957	8	9994.418	20
103.5	9468.914	3	9325.798	6	10128.519	17	9986.686	21
104.5	9462.913	-13	9318.521	-6	10121.988	6	9978.873	10
105.5	9456.871	-2	9311.207	10			9971.004	18
106.5	9450.752	0						
107.5	9444.570	9						
108.5	9438.294	-8						
109.5	9431.975	3			10081.282	-1	9930.514	-13
110.5	9425.572	-3			10074.246	9	9922.221	3
111.5	9419.102	-6			10067.122	7	9913.827	-9
112.5					10059.926	8	9905.369	-13
113.5							9896.861	7
114.5					10045.295	1	9888.254	-1
115.5					10037.874	5	9879.560	-21
116.5					10030.346	-21	9870.828	-7
117.5							9862.013	-2

stronger main bands. A compressed portion of the low resolution spectrum is presented in Fig. 1. The 1-0 band is the strongest band in our spectrum, and the 3-0 and 0-1 bands are weak because their intensities are affected by the 850 nm red pass filter and the band gap of the Si-photodiodes, respectively. The 3-0 band was too weak to be analyzed. All of the bands are degraded toward lower wavenumbers and the bandheads form in the R-branches.

The structure of each of these bands is very complex because of overlapping from different sub-bands. A Hund's case (a) ${}^4\Delta - {}^4\Delta$ transition consists of four main sub-bands, ${}^4\Delta_{1/2} - {}^4\Delta_{1/2}$, ${}^4\Delta_{3/2} - {}^4\Delta_{3/2}$, ${}^4\Delta_{5/2} - {}^4\Delta_{5/2}$, and ${}^4\Delta_{7/2} - {}^4\Delta_{7/2}$, which

are separated by twice the difference between the spin-orbit coupling constants of the upper and lower electronic states [$2(A' - A'')$]. At first glance, it is difficult to identify the bandheads of individual sub-bands, but a careful inspection of each band using a color Loomis-Wood program helped us to identify and assign the rotational structure. The Ω -assignments of the four sub-bands were initially based on the size of the Ω -doubling and were later confirmed by rotational analysis. The Ω -doubling is present mainly in the lower $a^4\Delta$ state and is largest for the ${}^4\Delta_{1/2}$ spin component. The ${}^4\Delta_{3/2}$ spin component has a smaller Ω -doubling and the ${}^4\Delta_{5/2}$ and ${}^4\Delta_{7/2}$ spin components show no splittings. The Ω -assignment

TABLE 5
Rotational Constants (in cm^{-1}) for the $a^4\Delta$ state of FeF

Const. ^a	$a^4\Delta_{7/2}$		$a^4\Delta_{5/2}$	
	$v=0$	$v=1$	$v=0$	$v=1$
T_{vv}	0.0	684.2032(27)	0.0	683.7856(36)
B_v	0.3892891(76)	0.3864504(91)	0.3909477(77)	0.3883694(97)
$10^7 \times D_v$	4.836(13)	4.868(16)	4.9761(71)	5.671(21)
$10^{12} \times H_v$	-0.525(61)	-0.563(81)	-0.389(26)	3.89(17)

Const.	$a^4\Delta_{3/2}$		$a^4\Delta_{1/2}$	
	$v=0$	$v=1$	$v=0$	$v=1$
T_{vv}	0.0	684.1789(38)	0.0	684.4777(26)
B_v	0.3924083(84)	0.3895014(83)	0.3938882(48)	0.3909613(49)
$10^7 \times D_v$	5.027(17)	5.023(17)	5.2807(40)	5.2713(36)
$10^{13} \times H_v$	-7.09(99)	-9.01(96)	1.91(10)	--
$10^3 \times p_v$	-0.977(48)	-0.496(52)	-7.404(36)	-9.215(84)
$10^7 \times p_{Dv}$	5.90(21)	3.53(23)	6.84(35)	8.98(44)
$10^{11} \times p_{Hv}$	-2.65(20)	0.35(21)	-3.11(14)	-6.81(25)

^aThe numbers in parentheses are one standard deviation in last two digits.

is also confirmed by the B_{eff} values in the different spin components with $B(^4\Delta_{7/2}) < B(^4\Delta_{5/2}) < B(^4\Delta_{3/2}) < B(^4\Delta_{1/2})$ as expected for an inverted $^4\Delta$ state. A schematic energy level diagram of this transition is presented in Fig. 2.

A compressed part of the 0–0 band of FeF is presented in Fig. 3 and the positions of the R -heads of the different sub-bands have been marked with arrows. The different sub-bands are not located in either increasing or decreasing order of Ω . The sub-band order in each vibrational band is $^4\Delta_{5/2}$ – $^4\Delta_{5/2}$, $^4\Delta_{3/2}$ – $^4\Delta_{3/2}$, $^4\Delta_{7/2}$ – $^4\Delta_{7/2}$, and $^4\Delta_{1/2}$ – $^4\Delta_{1/2}$ in order of decreasing wavenumbers. Evidently the simple spin–orbit energy level formula, $A\Lambda\Sigma$, fails for one or both of the $^4\Delta$ states. Since pure Δ states rarely display Ω -doubling, the lower $^4\Delta$ state is most probably interacting strongly with nearby states. This interaction (“Hund’s case (c) tendencies”) induces both a large Ω -doubling and irregular intervals between the spin components.

The structure of each of the four sub-bands consists of R and P branches consistent with the $\Delta\Omega = 0$ assignment. No Q -branches have been observed in any of the sub-bands and no transitions which violate the Hund’s case (a) selection rule $\Delta\Sigma = 0$ could be identified. This means that we are unable to measure any intervals between the spin components.

The R -head at $10\,423\text{ cm}^{-1}$ has been identified as the 0–0 band of the $7/2$ – $7/2$ sub-band. No Ω -doubling was

observed even for the highest J values. An interesting feature of this sub-band is the observation of perturbations in the lower $a^4\Delta$ state. The $v'' = 0$ vibrational level is perturbed near $J = 73.5$ and the $v'' = 1$ vibrational level is perturbed at $J = 61.5$. These perturbations affect both e and f parity components equally.

The 0–0 band with an R -head at $10\,447\text{ cm}^{-1}$ has been assigned to the $5/2$ – $5/2$ sub-band. An expanded portion of the 1–0 band of this sub-band near the R -head is presented in Fig. 4. The rotational structure consists of a single R and a single P branch, with almost identical intensity. Because of the overlapping from the returning lines of the R -branch after the formation of the head, the low J branch lines were not identified. The rotational analysis indicates that the $v'' = 0$ vibrational level of this sub-band is perturbed near $J = 55.5$. A similar perturbation has also been observed in the $v'' = 1$ vibrational level near $J = 36.5$. These perturbations affect both of the parity components by similar amounts.

The band with a 0–0 head located at $10\,433\text{ cm}^{-1}$ has been assigned to the $3/2$ – $3/2$ sub-band. The high J lines of this sub-band split into two components because of Ω -doubling. The rotational analysis indicates that perturbations affect mainly the lower $^4\Delta$ state. One perturbation which culminates at $J = 20.5$ affects all low J lines with $J < 33.5$ and these lines were excluded from the final fit.

TABLE 6
Rotational Constants (in cm^{-1}) for the $g^4\Delta$ state of FeF

Const. ^a	$g^4\Delta_{7/2}$			$g^4\Delta_{5/2}$		
	v=0	v=1	v=2	v=0	v=1	v=2
T_v	10418.6232(15)	10986.6997(12)	11548.7795(12)	10443.3833(12)	11013.2751(11)	11577.1764(13)
B_v	0.3557711(77)	0.3529176(77)	0.3500915(76)	0.3564175(80)	0.3535584(79)	0.3507325(72)
$10^7 \times D_v$	5.368(13)	5.340(13)	5.319(13)	5.3697(84)	5.3777(80)	5.4116(47)
$10^{13} \times H_v$	-3.46(62)	-3.67(66)	-4.04(60)	-4.91(35)	-3.70(34)	--

Const.	$g^4\Delta_{3/2}$			$g^4\Delta_{1/2}$		
	v=0	v=1	v=2	v=0	v=1	v=2
T_v	10428.9218(36)	10999.1775(36)	11563.4554(45)	10382.0712(12)	10951.6252(15)	11515.1623(12)
B_v	0.3572207(83)	0.3543172(88)	0.3514327(92)	0.3581057(48)	0.3551812(47)	0.3522900(48)
$10^7 \times D_v$	5.535(17)	5.517(18)	5.490(20)	5.6792(36)	5.6673(35)	5.6507(36)
$10^{13} \times H_v$	-1.70(98)	-1.8(10)	-2.4(12)	--	--	--
$10^7 \times p_{Dv}$	--	--	--	1.45(31)	3.24(31)	2.09(31)

^aThe numbers in parentheses are one standard deviation in last two digits.

The $1/2-1/2$ sub-band is weakest in intensity and the bandhead cannot be identified visually. In addition to its weak intensity, consistent with an inverted $^4\Delta$ excited state, this band is overlapped by the lines of all of the other sub-bands. Our Loomis–Wood program was essential in identifying the rotational lines. Perturbations have been observed in the $v' = 0$ and $v' = 2$ vibrational levels of the excited state of this sub-band. The observed perturbations affect only the f -parity levels at $J = 73.5$ and 65.5 in the $v' = 0$ and 2 vibrational levels, respectively.

The rotational assignments in the different bands were made by comparing combination differences for the common vibrational levels. It is difficult to make a definite e - and f -parity assignment in the bands with resolved Ω -doubling. The e - and f -parity assignments have been made arbitrarily. The observed $^4\Delta$ electronic states probably belong to Hund's case (a) coupling but the sub-bands were not fitted together. Rather than fitting all of the lines together with assumed constants we decided to use a simple Hund's case (c) term energy expression for each spin component:

$$\begin{aligned}
 F_v(J) = & T_v + B_v J(J+1) - D_v [J(J+1)]^2 \\
 & + H_v [J(J+1)]^3 \pm \frac{1}{2} [p_v (J + \frac{1}{2}) \\
 & + p_{Dv} (J + \frac{1}{2})^3 + p_{Hv} (J + \frac{1}{2})^5]
 \end{aligned}
 \quad [1]$$

Initially a band-by-band fit was obtained for each sub-

band. This fit provided similar constants for common vibrational levels from different bands, confirming their vibrational assignments. In the final fit, the lines of all of the vibrational bands in each sub-band were combined and fitted simultaneously. The observed lines positions for the $^4\Delta_{1/2}-^4\Delta_{1/2}$, $^4\Delta_{3/2}-^4\Delta_{3/2}$, $^4\Delta_{5/2}-^4\Delta_{5/2}$ and $^4\Delta_{7/2}-^4\Delta_{7/2}$ are provided in Tables 1, 2, 3, and 4, respectively, and the molecular constants for the lower and excited $^4\Delta$ states are provided in Tables 5 and 6, respectively.

RESULTS AND DISCUSSION

The $0-0$ FeF $^4\Delta-^4\Delta$ transition has sub-band origins at $10\,419\text{ cm}^{-1}$ ($7/2-7/2$), $10\,443\text{ cm}^{-1}$ ($5/2-5/2$), $10\,429\text{ cm}^{-1}$ ($3/2-3/2$), and $10\,382\text{ cm}^{-1}$ ($1/2-1/2$), while the corresponding FeH sub-bands occur at 9929 , $10\,026$, $10\,039$, and 9984 cm^{-1} . This close similarity between transition metal fluoride and hydride transitions has been noted by previous workers and was discussed by us for the CoF and CoH case (26, 25). In addition, there is a very high quality set of *ab initio* calculations for FeH (28) while the published FeF calculations are more primitive (8). It is, therefore, convenient to discuss the low-lying states of FeF in terms of the calculated FeH states (Fig. 5).

As noted by Pouilly *et al.* (8), the low-lying electronic states of FeF also correlate directly to the states of the Fe^+ atom. This means that the energy levels of FeF, FeH, and Fe^+ share a remarkably similar pattern. The F^- and H^-

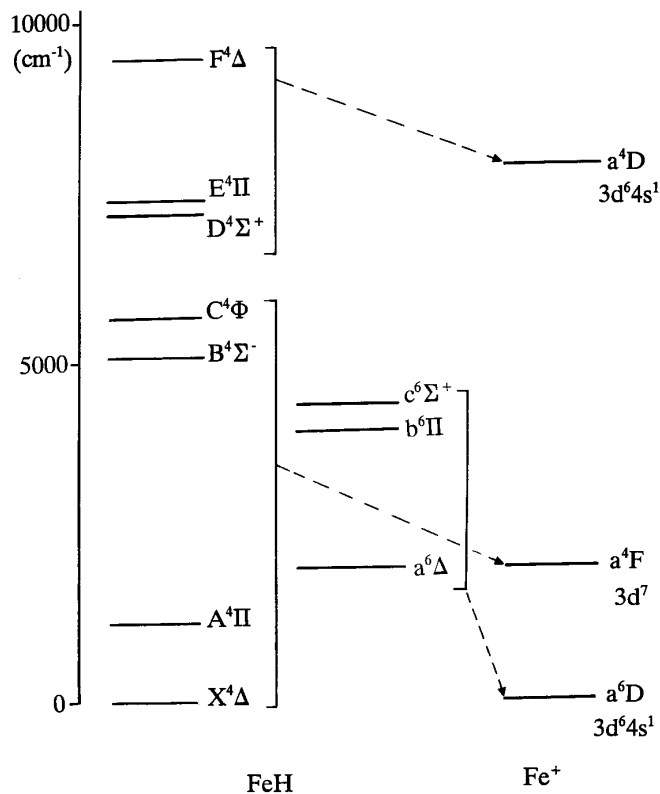


FIG. 5. The correlation between the calculated (28) electronic energy levels of FeH and the atomic energy levels of Fe^+ .

ligand fields thus give similar energy level patterns in FeF and FeH, although the bonding in FeH is expected to be much more covalent than that in FeF.

The lowest energy term of the Fe^+ atom is a^6D , which arises from the $3d^64s^1$ configuration (37). This 6D term correlates to the $a^6\Delta$, $b^6\Pi$, and $c^6\Sigma^+$ states in FeH (Fig. 5). The first excited term in Fe^+ is a^4F at 2417 cm^{-1} , arising from the $3d^7$ configuration (37). The FeH molecular states correlating to a^4F are $X^4\Delta$, $A^4\Pi$, $B^4\Sigma^-$, and $C^4\Phi$ (Fig. 5). The $X^4\Delta$ ground state of FeH thus correlates with the first excited a^4F term of Fe^+ . The third Fe^+ term, $a^4D(3d^64s^1)$, correlates with the $D^4\Sigma^+$, $E^4\Pi$, and $F^4\Delta$ states of FeH.

The *ab initio* prediction of the energy ordering of the low-lying electronic states of FeH is a very challenging problem. Large basis sets and an extensive treatment of electron correlation are necessary to get a ${}^4\Delta$ ground state rather than the "expected" ${}^6\Delta$ state which correlates to the Fe^+a^6D ground state term. In particular, the inclusion of electron correlation lowers the energy of the ${}^4\Delta$ state (Fe^+ , 4F , $3d^7$) more than the ${}^6\Delta(\text{Fe}^+$, 6D , $3d^64s^1$) state and switches the energy ordering of the two states. While the general picture of the low-lying states of FeH is easily predicted from the Fe^+ energy levels, the detailed ordering of the FeH states is clearly a sensitive function of many effects.

The ground state of FeF is known to be $X^6\Delta$ on the basis

of both experimental observations and theoretical calculations. Thus for FeF, the "expected" ordering of the lowest energy ${}^4\Delta$ and ${}^6\Delta$ states is found. In view of the similarities between the FeF and FeH spectra as found in our work and the different effects of electron correlation on states originating from Fe^+3d^7 and $3d^64s$ configurations, we expect that the sextet manifold will be lowered in energy relative to the quartet manifold in FeF as compared to FeH. We expect (and hope!) that the energy ordering within the quartet and sextet manifolds will be qualitatively the same in FeH and FeF. The energy ordering of the low-lying states of FeF will then be as shown in Fig. 6. Of course, some of the details in Fig. 6 may be in error but a high quality *ab initio* calculation as well as additional experiments are necessary to confirm or refute Fig. 6. On the basis of Fig. 6, the observed FeF transition at $1\ \mu\text{m}$ is thus $g^4\Delta$ - $a^4\Delta$.

The main problem with using a Hund's case (c) energy level expression for each of the four spin components of a ${}^4\Delta$ state is the determination of "true" Hund's case (a) molecular constants from the effective constants of the fit. A simple perturbation theory analysis of the 4×4 matrix representation of the energy levels of a ${}^4\Delta$ state leads to the following relationships:

$$B_{\text{eff}}(7/2) = B(1 + 3B/2A) \quad [2(a)]$$

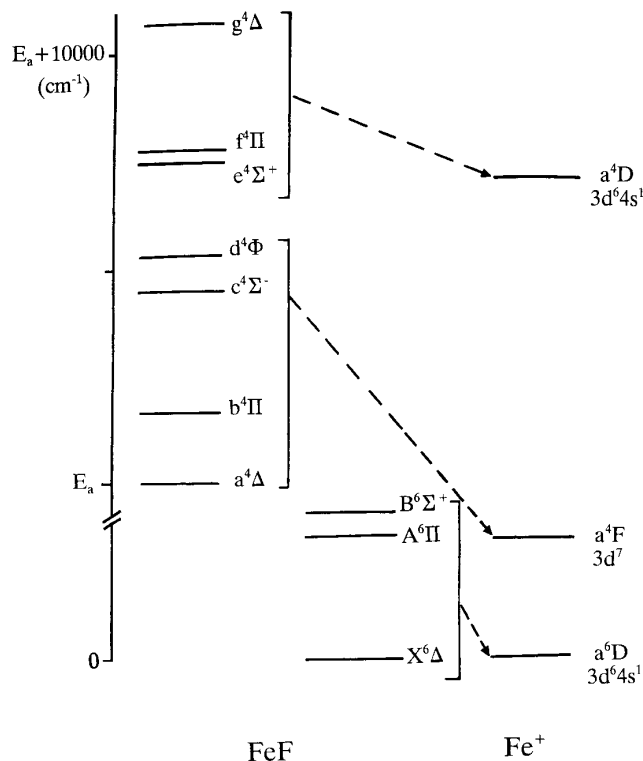


FIG. 6. A qualitative energy level diagram for FeF based on the calculated energy levels of FeH. Note the correspondence between the atomic Fe^+ and the molecular FeF energy levels.

$$B_{\text{eff}}(5/2) = B(1 + B/2A) \quad [2(b)]$$

$$B_{\text{eff}}(3/2) = B(1 - B/2A) \quad [2(c)]$$

$$B_{\text{eff}}(1/2) = B(1 - 3B/2A). \quad [2(d)]$$

In these equations A is the usual spin-orbit coupling constant and B is the "true" rotational constant associated with the ${}^4\Delta$ state. A quick check using Eqs. [2(a)]–[2(d)] leads to the conclusion that both the $g^4\Delta$ and $a^4\Delta$ states are inverted ($A < 0$). These equations [2(a)]–[2(d)] work surprisingly well considering that the sub-band origins are so irregular. For example, for $v = 0$ in the $a^4\Delta$ state $B_{\text{eff}}(7/2) - B_{\text{eff}}(5/2) = -0.00166 \text{ cm}^{-1}$, $B_{\text{eff}}(5/2) - B_{\text{eff}}(3/2) = -0.00146 \text{ cm}^{-1}$, and $B_{\text{eff}}(3/2) - B_{\text{eff}}(1/2) = -0.00148 \text{ cm}^{-1}$ which gives $B''_0 = 0.3916 \text{ cm}^{-1}$ and $A''_0 = -100 \text{ cm}^{-1}$ by simple averaging. For the excited $g^4\Delta$ state $B'_0 = 0.3569 \text{ cm}^{-1}$ and $A_0 = -164 \text{ cm}^{-1}$.

The equilibrium internuclear separation r_e was found by using effective B_0 and B_1 values for each spin component to calculate effective B_e values and then averaging them to obtain a "true" B_e value. Using this algorithm for the $a^4\Delta$ state gives $B_e = 0.3930 \text{ cm}^{-1}$, $\alpha_e = 0.0028 \text{ cm}^{-1}$, and $r_e = 1.7392 \text{ \AA}$, while for the $g^4\Delta$ state $B_e = 0.3583 \text{ cm}^{-1}$, $\alpha_e = 0.0029 \text{ cm}^{-1}$, and $r_e = 1.8412 \text{ \AA}$. Averaging the $\Delta G(1/2)$ values results in $\Delta G''(1/2) = 684.16(25) \text{ cm}^{-1}$ and $\Delta G'(1/2) = 569.44(83) \text{ cm}^{-1}$.

CONCLUSIONS

The near infrared emission spectrum of FeF has been observed at high resolution using a Fourier transform spectrometer. The bands observed in the $9000\text{--}12\,000 \text{ cm}^{-1}$ region have been assigned as the $0\text{--}1$, $0\text{--}0$, $1\text{--}0$, and $2\text{--}0$ bands of a new $g^4\Delta\text{--}a^4\Delta$ transition. A rotational analysis of these bands has been made and the molecular constants have been determined. This FeF transition is analogous to the $F^4\Delta\text{--}X^4\Delta$ transition of FeH (30) observed near $1 \mu\text{m}$. The similarity between the electronic energy levels of FeF, FeH, and Fe^+ has been discussed.

ACKNOWLEDGMENTS

We thank J. Wagner and C. Plymate of the National Solar Observatory for assistance in obtaining the spectra. The National Solar Observatory is operated by the Association of Universities for Research in Astronomy, Inc., under contract with the National Science Foundation. The research described here was supported by funding from the NASA laboratory astrophysics program. Some support was also provided by the Petroleum Research Fund, administered by the American Chemical Society, and the Natural Sciences and Engineering Research Council of Canada.

REFERENCES

1. B. Rosen, "Spectroscopic Data Relative to Diatomic Molecules." Pergamon, Oxford, 1970.
2. W. E. Jones and G. Krishnamurty, *J. Phys. B* **13**, 3375–3382 (1980).
3. E. A. Shenyavskaya, A. J. Ross, A. Topouzhanian, and G. Wannous, *J. Mol. Spectrosc.* **162**, 327–334 (1993).
4. O. Launila, *J. Mol. Spectrosc.* **169**, 373–395 (1995).
5. B. Simard and O. Launila, *J. Mol. Spectrosc.* **168**, 567–578, (1994).
6. O. Launila, B. Simard, and A. M. James, *J. Mol. Spectrosc.* **159**, 161–174, (1993).
7. B. Pouilly, J. Schamps, D. J. W. Lumley, and R. F. Barrow, *J. Phys. B* **11**, 2281–2287 (1978).
8. B. Pouilly, J. Schamps, D. J. W. Lumley, and R. F. Barrow, *J. Phys. B* **11**, 2289–2299 (1978).
9. A. G. Adam, L. P. Fraser, W. D. Hamilton, and M. C. Steeves, *Chem. Phys. Lett.* **230**, 82–86 (1994).
10. R. S. Ram, P. F. Bernath, and S. P. Davis, *J. Mol. Spectrosc.* **173**, 158–176 (1995).
11. C. Dufour, I. Hikmet, and B. Pinchemel, *J. Mol. Spectrosc.* **165**, 398–405 (1994).
12. T. S. Steimle, C. R. Brazier, and J. M. Brown, *J. Mol. Spectrosc.* **110**, 39–52 (1985).
13. R. K. Brinton and A. B. Callear, *J. Chem. Soc. Faraday Trans. 2* **70**, 203–214 (1974).
14. J. B. West and H. P. Broida, *J. Chem. Phys.* **62**, 2566–2574 (1975).
15. M. D. Allen and L. M. Ziurys, submitted for publication.
16. L. N. Gorokhov, M. Yu. Ryzhov, and Yu. S. Khodeev, *Russ. J. Phys. Chem.* **59**, 1761–1764 (1985).
17. J. M. Delaval, C. Dufour, and J. Schamps, *J. Phys. B* **13**, 4757–4769 (1980).
18. J. M. Delaval and J. Schamps, *J. Phys. B* **15**, 4137–4149 (1982).
19. M. Tanimoto, S. Saito, and T. Okabayashi, *Chem. Phys. Lett.* **242**, 153–156 (1995).
20. J. Cernicharo and M. Guelin, *Astron. Astrophys.* **183**, L10–L12 (1987).
21. L. M. Ziurys, A. J. Apponi, and T. G. Phillips, *Astrophys. J.* **433**, 729–732 (1994).
22. R. F. Wing, J. Cohen, and J. W. Brault, *Astrophys. J.* **216**, 659–664 (1977).
23. R. E. S. Clegg and D. L. Lambert, *Astrophys. J.* **226**, 931–936 (1978).
24. A. Jorissen, V. V. Smith, and D. L. Lambert, *Astron. Astrophys.* **261**, 164–187 (1992).
25. R. S. Ram and P. F. Bernath, *J. Mol. Spectrosc.* **175**, 1–6 (1996).
26. R. S. Ram, P. F. Bernath, and S. P. Davis, *J. Chem. Phys.* **104**, 6949–6955 (1996).
27. M. Krauss and W. J. Stevens, *J. Chem. Phys.* **82**, 5584–5596 (1985).
28. S. R. Langhoff and C. W. Bauschlicher, Jr., *J. Mol. Spectrosc.* **141**, 243–257 (1990).
29. M. Sodupe, J. M. Lluch, A. Oliva, F. Illas, and J. Rubio, *J. Chem. Phys.* **92**, 2478–2480 (1990).
30. J. G. Phillips, S. P. Davis, B. Lindgren, and W. J. Balfour, *Astrophys. J. Suppl.* **65**, 721–778 (1987).
31. J. P. Towle, J. M. Brown, K. Lipus, E. Bachem, and W. Urban, *Mol. Phys.* **79**, 835–845 (1993).
32. R. T. Carter, T. C. Steimle, and J. M. Brown, *J. Chem. Phys.* **99**, 3166–3173 (1993).
33. R. T. Carter and J. M. Brown, *J. Chem. Phys.* **101**, 2699–2709 (1994).
34. W. J. Balfour, B. Lindgren, and S. O'Connor, *Phys. Scrip.* **28**, 551–560 (1983).
35. J. G. Phillips and S. P. Davis, *Astrophys. J. Suppl.* **66**, 227–232 (1988).
36. D. Cerny, R. Bacis, G. Guelachvili, and F. Roux, *J. Mol. Spectrosc.* **73**, 154–167 (1978) and private communication.
37. C. E. Moore, "Atomic Energy Levels," Vol. II, National Bureau of Standards, 1958.